

The Pennsylvania State University

The Graduate School

Department of Biochemistry, Microbiology and Molecular Biology

**INVESTIGATION OF IRON-SULFUR CLUSTER INVOLVEMENT IN
CATALYSIS BY THE HYDRO-LYASE QUINOLINATE SYNTHASE**

A Thesis in

Biochemistry, Microbiology and Molecular Biology

by

Amy E. Griffiths

© 2008 Amy E. Griffiths

Submitted in Partial Fulfillment
of the Requirements
for the Degree of

Master of Science

August 2008

The thesis of Amy E. Griffiths was reviewed and approved* by the following:

Squire J. Booker
Associate Professor of Chemistry
Associate Professor of Biochemistry and Molecular Biology
Thesis Advisor

Carsten Krebs
Associate Professor of Chemistry
Associate Professor of Biochemistry and Molecular Biology

Katsuhiko S. Murakami
Assistant Professor of Biochemistry and Molecular Biology

Mary Beth Williams
Associate Professor of Chemistry

Richard J. Frisque
Professor of Biochemistry and Molecular Biology
Head of the Department of Biochemistry, Microbiology and Molecular
Biology

*Signatures are on file in the Graduate School

ABSTRACT

Quinolinate synthase catalyzes the formation of quinolinic acid, a key intermediate in the biosynthesis of the cofactor nicotinamide adenine dinucleotide. In prokaryotes, quinolinic acid is synthesized via the concerted action of two enzymes, L-aspartate oxidase, and quinolinate synthase (NadA). L-aspartate oxidase, a flavin-dependent enzyme that converts L-aspartic acid to iminoaspartate, has been well-characterized. In contrast, few studies have been conducted on NadA, which catalyzes a condensation reaction between iminoaspartate and dihydroxyacetone phosphate to form quinolinic acid. Recent work has found that *Escherichia coli* NadA contains a $[4\text{Fe-}4\text{S}]^{2+}$, and that this cluster may serve a direct role in catalysis. Further support for the role of the iron-sulfur cluster in catalysis is established here through investigations of NadA from *E. coli*, *Mycobacterium tuberculosis*, and *Pyrococcus horikoshii*.

While initial work with *E. coli* NadA has established the presence of an iron-sulfur cluster, this work indicates its necessity for catalysis. Isolation of a cluster-less apoprotein is described, and subsequent spectroscopic and activity analysis of the apoprotein indicates that it is in fact unable to catalyze the formation of quinolinic acid. Additionally, the cluster can be chemically reconstituted in this form of the protein, yielding a catalytically active form of NadA, with characteristics nearly identical to the holoprotein previously described.

An understanding of NadA from *M. tuberculosis* could be of use in designing new antimicrobial drugs to combat this deadly human pathogen. Although the *M. tuberculosis*

NadA sequence does not contain the CX₂CX₂C motif that is commonly found in 4Fe-4S enzymes it does possess an iron-sulfur cluster similar to that in *E. coli*.

A recent report of the crystal structure of NadA from the archeon *P. horikoshii* describes catalytic activity of the protein in the absence of an iron-sulfur cluster. To reproduce this observation independently, the *P. horikoshii nadA* gene was cloned and the protein purified under anaerobic conditions. The isolated protein did in fact contain a [4Fe-4S]²⁺ cluster in its catalytically active form, while apoprotein, or protein isolated under aerobic conditions showed no activity. The lack of cluster in the previously reported structure is believed to result from oxygen exposure. To gain further understanding of this enzyme and the role of its cluster in catalysis, studies were initiated to obtain a crystal structure of the protein with an intact cluster.

TABLE OF CONTENTS

| | |
|--|-----|
| LIST OF ABBREVIATIONS..... | vii |
| LIST OF FIGURES | ix |
| LIST OF TABLES..... | xi |
| ACKNOWLEDGEMENTS..... | xii |
| CHAPTER 1: Introduction | 1 |
| 1.1 Biosynthesis of Nicotinamide Adenine Dinucleotide..... | 1 |
| 1.1.a Investigations of L-Aspartate Oxidase | 5 |
| 1.1.b Investigations of Quinolinate Synthase | 5 |
| 1.2 Iron-Sulfur Cluster Hydrolyases..... | 6 |
| 1.2.a Aconitase..... | 8 |
| 1.2.b Dihydroxy-acid Dehydratase..... | 10 |
| 1.2.c Serine Dehydratase..... | 10 |
| 1.2.d Quinolinate Synthase..... | 11 |
| 1.3 Proposed Mechanisms of the Quinolinate Synthase Reaction..... | 12 |
| 1.4 Crystal Structure of Quinolinate Synthase..... | 16 |
| 1.5 Specific Aims..... | 17 |
| 1.6 References..... | 17 |
| CHAPTER 2: The <i>Escherichia coli</i> Quinolinate Synthase [4Fe-4S] Cluster Is Required for Catalysis..... | 21 |
| 2.1 Introduction..... | 21 |
| 2.2 Materials and Methods..... | 22 |

| | |
|--|----|
| 2.3 Results..... | 30 |
| 2.4 Discussion..... | 35 |
| 2.5 References..... | 37 |
| | |
| CHAPTER 3: Purification and Characterization of <i>Mycobacterium tuberculosis</i> Quinolate Synthase..... | 40 |
| 3.1 Introduction..... | 40 |
| 3.2 Materials and Methods..... | 41 |
| 3.3 Results..... | 52 |
| 3.4 Discussion..... | 58 |
| 3.5 References..... | 59 |
| | |
| CHAPTER 4: Cloning, Purification and Characterization of <i>Pyrococcus horikoshii</i> Quinolate Synthase..... | 62 |
| 4.1 Introduction..... | 62 |
| 4.2 Materials and Methods..... | 64 |
| 4.3 Results..... | 72 |
| 4.4 Discussion..... | 81 |
| 4.5 References..... | 85 |

LIST OF ABBREVIATIONS

| | |
|--------|--|
| AI | as-isolated |
| DHAP | dihydroxyacetone phosphate |
| DLS | dynamic light scattering |
| DTT | dithiothreitol |
| ENDOR | electron nuclear double resonance |
| EPR | electron paramagnetic resonance |
| FAD | flavin adenine dinucleotide |
| Fe/S | iron–sulfur |
| G3P | glyceraldehyde 3-phosphate |
| HEPES | <i>N</i> -(2-hydroxyethyl)piperazine- <i>N'</i> -(2-ethanesulfonic acid) |
| HPLC | high-performance liquid chromatography |
| IA | iminoaspartate |
| IMAC | immobilized metal affinity chromatography |
| IS | internal standard |
| LB | Luria–Bertani |
| MOPS | 3-(<i>N</i> -morpholino) propane-sulfonic acid |
| NAD | nicotinamide adenine dinucleotide |
| NADP | nicotinamide adenine dinucleotide phosphate |
| NadA | quinolinate synthase |
| NadB | L-aspartate oxidase |
| Ni-NTA | nickel nitrilotriacetic acid |

| | |
|----------------|--|
| OAA | oxaloacetate |
| P _i | inorganic phosphate |
| PCR | polymerase chain reaction |
| PMSF | phenylmethanesulfonyl fluoride |
| QA | quinolinic acid |
| RCN | reconstituted |
| SDS-PAGE | sodium dodecylsulfate-polyacrylamide gel electrophoresis |
| WT | wild-type |

LIST OF FIGURES

| | |
|---|----|
| Figure 1-1: Structure of nicotinamide adenine dinucleotide..... | 2 |
| Figure 1-2: Nicotinamide adenine dinucleotide biosynthetic pathways..... | 4 |
| Figure 1-3: Reaction catalyzed by aconitase..... | 8 |
| Figure 1-4: Substrate binding to iron-sulfur cluster of aconitase..... | 9 |
| Figure 1-5: Reaction catalyzed by dihydroxy-acid dehydratase..... | 10 |
| Figure 1-6: Deamination of L-serine..... | 11 |
| Figure 1-7: Reaction catalyzed by quinolinate synthase..... | 12 |
| Figure 1-8: Proposed mechanisms of quinolinic acid formation..... | 15 |
| Figure 1-9: Proposed mode of quinolinic acid precursor binding to cluster..... | 16 |
| Figure 2-1: SDS-PAGE of <i>E. coli</i> NadA apoprotein expression..... | 31 |
| Figure 2-2: SDS-PAGE of <i>E. coli</i> NadA apoprotein purification..... | 32 |
| Figure 2-3: UV-visible spectra of Apo-NadA from <i>E. coli</i> | 33 |
| Figure 2-4: Activity assay of Apo-NadA from <i>E. coli</i> | 34 |
| Figure 2-5: EPR spectra of Apo-NadA from <i>E. coli</i> | 35 |
| Figure 3-1: SDS-PAGE of <i>M. tuberculosis</i> NadA expression..... | 52 |
| Figure 3-2: SDS-PAGE of WT <i>M. tuberculosis</i> NadA purification..... | 54 |
| Figure 3-3: UV-visible spectra of WT <i>M. tuberculosis</i> NadA..... | 54 |
| Figure 3-4: Mössbauer spectrum of ^{57}Fe <i>M. tuberculosis</i> NadA..... | 55 |
| Figure 3-5: EPR spectrum of <i>M. tuberculosis</i> NadA..... | 56 |
| Figure 3-6: SDS-PAGE of C114A <i>M. tuberculosis</i> NadA purification..... | 57 |

| | |
|---|----|
| Figure 4-1: Sequence alignment of <i>E. coli</i> and <i>P. horikoshii</i> quinolinate synthases.... | 64 |
| Figure 4-2: SDS-PAGE of <i>P. horikoshii</i> NadA expression..... | 73 |
| Figure 4-3: SDS-PAGE of <i>P. horikoshii</i> NadA purification..... | 74 |
| Figure 4-4: UV-visible spectra of WT <i>P. horikoshii</i> NadA..... | 75 |
| Figure 4-5: Mössbauer spectra of as-isolated ⁵⁷ Fe <i>P. horikoshii</i> NadA..... | 77 |
| Figure 4-6: EPR Spectrum of reduced as-isolated ⁵⁷ Fe <i>P. horikoshii</i> NadA..... | 77 |
| Figure 4-7: UV-visible spectra of Apo-NadA from <i>P. horikoshii</i> | 79 |
| Figure 4-8: Activity assay of Apo-NadA from <i>P. horikoshii</i> | 79 |
| Figure 4-9: Average diameter plot obtained from DLS of <i>P. horikoshii</i> NadA..... | 80 |
| Figure 4-10: Crystal of <i>P. horikoshii</i> NadA..... | 81 |

LIST OF TABLES

| | |
|---|----|
| Table 1-1: Hydro-lyase Enzymes Containing Fe/S Clusters with Purported Catalytic Roles..... | 7 |
| Table 3-1: Primers used in cloning and mutagenesis of <i>nadA</i> genes from <i>M. tuberculosis</i> | 45 |

ACKNOWLEDGEMENTS

First and foremost, I owe a thank you to my advisor, Dr. Squire Booker. His intelligence, patience and sense of humor have made working for him a wonderful experience. I also thank ‘The Trifecta’ – Drs. Squire Booker, Marty Bollinger and Carsten Krebs. Their collective energy and enthusiasm for their science brought me to Penn State, impressed me while I was here, and is something I will aspire to achieve in the future. My past and present committee members, Drs. Squire Booker, Marty Bollinger, Carsten Krebs, Katsu Murakami, and Mary Beth Williams, have also been great over the past few years, and Neela Yennawar has been indispensable in the logistics and trouble-shooting of the recent crystallography project.

In the lab, Drs. Robert Cicchillo and David Iwig got me started, kept me questioning, and taught me to have a little fun. Allison Saunders has been a fantastic lab partner since our first days in the lab, I never would have made it as far as I did without your help. Liz Billgren and Tyler Grove added unique perspectives to experimental and office debates. Liz, thank you for all of your help wrapping things up near the end, and I wish you luck in your future endeavors. And to Kyunghoon Lee, technical tour-de-force, yet always ready to “take a break”, for his calm reasoning, listening to my ranting, teaching me all of the molecular biology I know, and for always being there. I regret that I was not able to work with this group longer, wish you the best, and look forward to hearing of your future achievements.

Outside the lab, I thank my family for the independence they have encouraged me to have, and my sister for her support. For creating a home for me to come home to at

the end of long lab days, I thank Dr. Ebru Ersay and also Eric Roman, who has kept me grounded by sharing his artistic images, random trivia, bargain buys, calming presence, inimitable perceptions of the world, and Pepper. Finally, thanks to soon-to-be doctor Jennifer Newell, for her constant optimism, encouragement, companionship on weekend escapes from grad. school, photo-documentation of the last eight years, and for setting the bar high, forging the way, and then allowing me to attempt to follow in her footsteps.

Chapter 1:

Introduction

Quinolinate synthase catalyzes the synthesis of quinolinic acid, a key intermediate in the prokaryotic pathway forming nicotinamide adenine dinucleotide. It is a member of the hydro-lyase family of enzymes [EC 4.2.1.x], which catalyzes the removal of a proton and hydroxyl group from their substrates, creating a carbon-carbon double bond. A number of hydro-lyases have been shown to contain a [4Fe-4S] cluster that is believed to play a key role in the mechanism of catalysis. It is proposed that the [4Fe-4S] cluster in quinolinate synthase will function as a Lewis acid, providing an open coordination site to which the hydroxyl group of the substrate binds and is activated for elimination in the last step of the reaction, as seen in aconitase, the most studied member of the cluster-containing hydro-lyases.

1.1 Biosynthesis of Nicotinamide Adenine Dinucleotide

Nicotinamide adenine dinucleotide (NAD) is an essential cofactor found throughout biological systems. It consists of two nucleotides, one containing the nicotinamide functionality at its 1' position, the other containing adenine at this position, linked through a pair of bridging phosphate groups at the 5' carbon (Figure 1-1). NAD is best recognized for its role in myriad oxidation-reduction reactions, in which it can donate or accept a hydride from its nicotinamide group. Additionally, NAD has been shown to play a role in a number of non-redox reactions, including ADP-ribosylation,

histone deacetylation, calcium signaling, DNA repair, and regulation of cell death and aging [1, 2]. More recently, NAD involvement has been indicated in protective mechanisms against neurodegenerative diseases such as Alzheimer's disease, Parkinson's disease, and multiple sclerosis [2]. NAD kinase can also convert NAD into nicotinamide adenine dinucleotide phosphate (NADP), a cofactor with similar chemical properties, which serves in a number of additional metabolic roles.

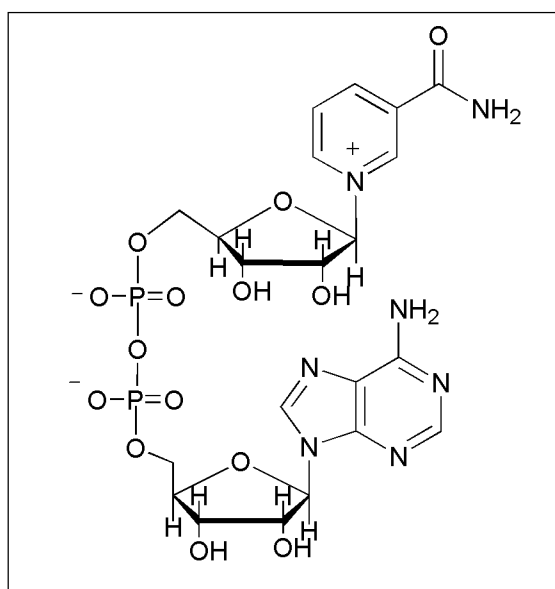


Figure 1-1: Structure of nicotinamide adenine dinucleotide

Nicotinamide adenine dinucleotide is formed *de novo* through two distinct biosynthetic pathways: in most eukaryotes, synthesis originates with the amino acid L-tryptophan and proceeds through eight enzymatic steps and requires oxygen as a cosubstrate, and most prokaryotes utilize an anaerobic pathway beginning with L-aspartate. While the initial steps of these two pathways differ significantly, their final steps, from the intermediate quinolinic acid (QA) to NAD, are identical (Figure 1-2).

The differences between the two pathways suggest that an understanding of the prokaryotic system is of interest because it could form the foundation for the design of new antimicrobial agents.

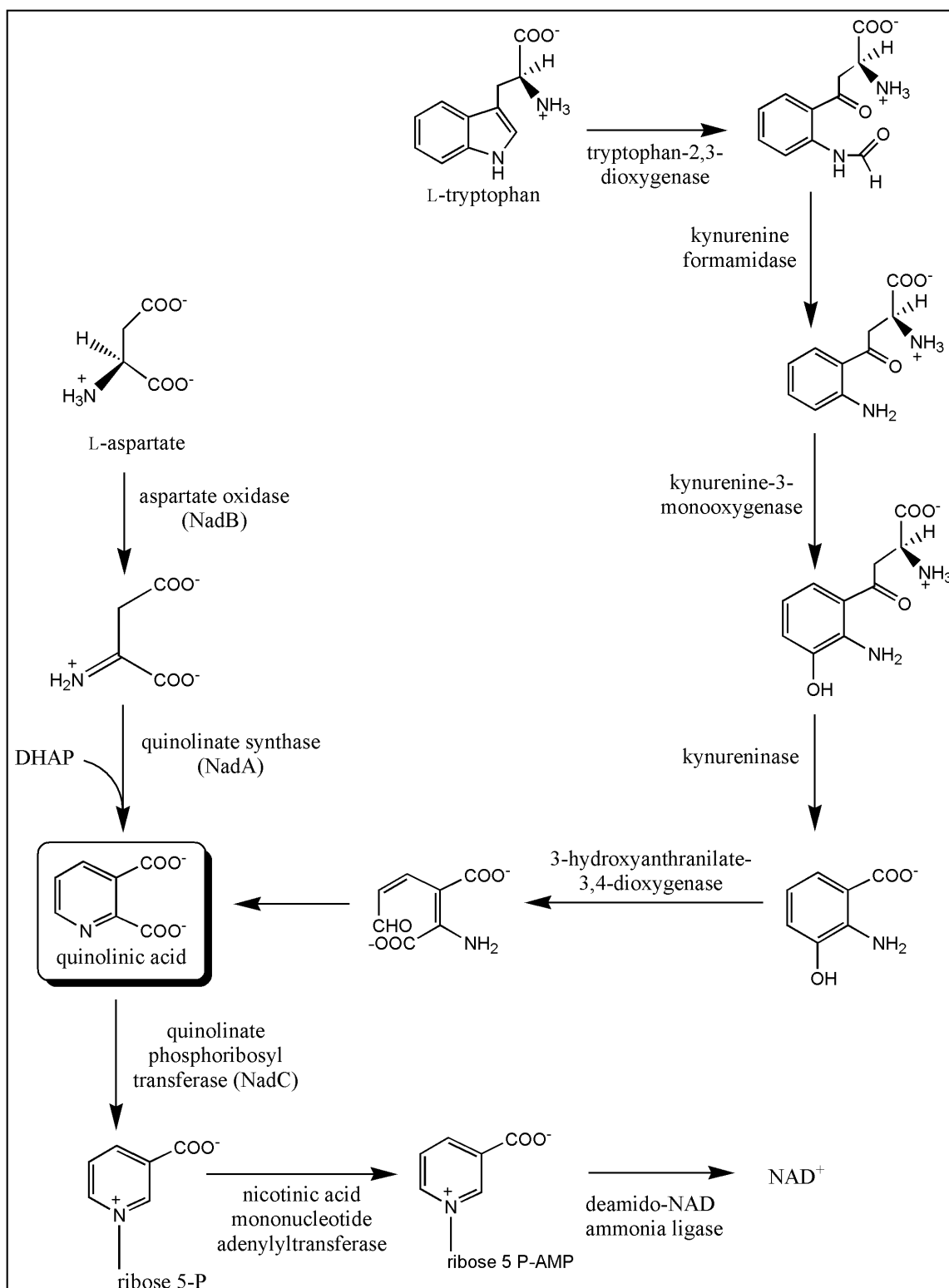


Figure 1-2: Nicotinamide adenine dinucleotide biosynthetic pathways

Beginning with L-aspartate, two enzymatic steps are required to form quinolinic acid in prokaryotes. The flavin-dependent enzyme, L-aspartate oxidase, or NadB, catalyzes a two-electron oxidation of the substrate, forming iminoaspartate (IA) in the first step of the pathway. Quinolinate synthase, or NadA, then performs a condensation reaction between iminoaspartate and dihydroxyacetone phosphate, forming QA. The work of Gholson demonstrated that the NadB protein preceded the NadA protein in the pathway, and confirmed the identity of the NadB product, iminoaspartate, by substituting chemically generated iminoaspartate for the NadB enzyme [3]. Iminoaspartate is unstable, with a half-life of 2.5 minutes at 37 °C and pH 8.0, suggesting that NadB and NadA may form a complex in order to utilize iminoaspartate efficiently [3].

1.1.a Investigations of L-Aspartate Oxidase

NadB is a 60 kDa protein that contains one molecule of flavin adenine dinucleotide (FAD) per polypeptide [4]. The crystal structure of *E. coli* NadB displays a capping region over the active site of the protein which is open in the apo-form and closed in the flavin adenine dinucleotide (FAD)-bound holo-form [5]. Upon oxidation of L-aspartate to IA, the cofactor is reduced to FADH₂. The cofactor may be restored to its catalytically active state after oxidation by molecular oxygen, affording hydrogen peroxide. Under anaerobic conditions, fumarate can be substituted as an electron donor, which is then converted to succinate.

1.1.b Investigations of Quinolinate Synthase

In contrast to NadB, quinolinate synthase has only recently become a focus of research study. The labile activity of the enzyme, in addition to a CXXCXXC motif in its primary structure, suggested that the protein could contain an oxygen sensitive iron-sulfur

cluster [6, 7]. The first purification to homogeneity was reported in 1999 by Ceciliani et al, who overexpressed the *nadA* gene, and then renatured and refolded ~38.2 kDa protein from inclusion bodies [8]. Shortly thereafter, purification of the protein under anaerobic conditions, followed by quantification of iron and sulfide, activity analysis, and UV-visible, electron paramagnetic resonance (EPR) and Mössbauer spectroscopies confirmed that NadA does in fact contain one $[4\text{Fe-4S}]^{2+}$ cluster per protein, and that the cluster is required for turnover [9, 10]. The requirement for the iron-sulfur cluster in catalysis of a dehydration mechanism places quinolinate synthase among the cluster-containing hydro-lyases, a family of enzymes typified by aconitase.

1.2 Iron-sulfur cluster Hydro-lyases

Protein-bound iron-sulfur clusters have long been known for their role in electron transfer. More recently, they have been shown to serve additional roles, including regulatory, structural, and catalytic functions. A number of hydro-lyase proteins that are purported to utilize an iron-sulfur cluster in catalysis are described in Flint and Allen's review, "Iron-Sulfur Proteins with Nonredox Functions," and listed in Table 1-1 [11]. While many of these enzymes have not been extensively characterized, the best studied are quinolinate synthase, serine deaminase, and aconitase, which serves as the paradigm for the iron-sulfur containing hydro-lyases.

| |
|--|
| <u>Catalytic Functions</u> |
| Aconitase |
| Homoaconitase |
| Methylcitrate Dehydratase |
| 2-Methylisocitrate Dehydratase |
| Isopropylmalate Isomerase |
| Fumarase A and B |
| Maleate Hydratase |
| Dimethylmaleate Hydratase |
| Mesaconase |
| Citraconase |
| Tartrate Dehydratase |
| Dihydroxy-acid Dehydratase |
| Phosphogluconate Dehydratase |
| Serine Dehydratase |
| Quinolate Synthase |
| Gluconate, Mannonate, Altronate, and Fuconate Dehydratases |
| <u>Catalytic and Redox Functions</u> |
| (2 <i>R</i>)-Lactyl-CoA Dehydratase |
| 2-(2 <i>R</i>)-Hydroxyglutaryl-CoA Dehydratase |

Table 1-1: Hydro-lyase Enzymes Containing Fe/S Clusters with Purported Catalytic Roles¹¹

1.2.a Aconitase

Aconitase catalyzes the interconversion of citrate and isocitrate via the intermediate *cis*-aconitate, which must undergo a 180 degree rotation in order for the reaction to proceed. Thus, this unique enzyme catalyzes 4 stereospecific reactions: the dehydration of citrate to *cis*-aconitate, the rehydration of *cis*-aconitate to isocitrate, the dehydration of isocitrate to *cis*-aconitate, and the rehydration of *cis*-aconitate to citrate (Figure 1-3).

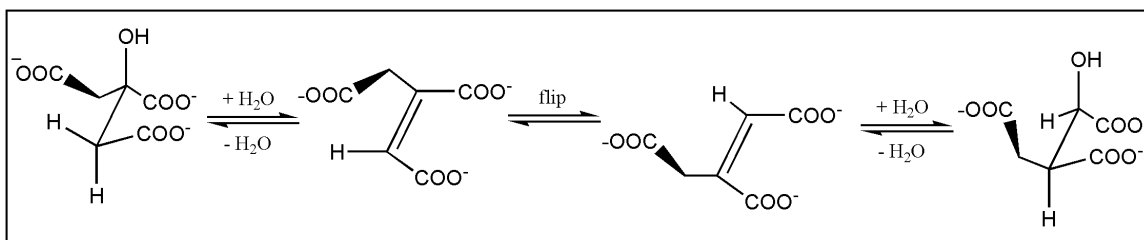


Figure 1-3: Reaction catalyzed by aconitase

Despite the complexities of the enzymatic reaction, aconitase has been studied in depth through a number of biochemical, kinetic, crystallographic and spectroscopic approaches that have resulted in a detailed understanding of this enzyme [12]. An initial observation was that enzyme activity was lost on purification, but could be recovered by addition of iron and a reductant [13]. The use of EPR, Mössbauer, and electron nuclear double resonance (ENDOR) spectroscopy were particularly useful in establishing the nature of the metallocofactor and its role in the reaction, which was later confirmed by crystal structures of aconitase with bound substrate and substrate analogs [14, 15]. Surprisingly, the crystal structures indicate that an active site serine residue plays a key role in the mechanism, acting as the base that abstracts the proton from either citrate or

isocitrate to form the cis-aconitate intermediate. The extensive research done on aconitase has led to the development of the aconitase paradigm [11]. Several of the tenets of the paradigm are as follows:

- (1) Aconitase contains a $[4\text{Fe-4S}]^{2+,+}$ cluster that is required for catalysis.
- (2) Three of the iron atoms in the cluster have ligands from the protein; the fourth iron, termed Fe_a , is bound to a hydroxyl group in its substrate-free form, and to a water molecule and the hydroxyl and carboxyl groups of substrate when either isocitrate or citrate are bound (Figure 1-4).
- (3) The role of the Fe-S cluster is to act as a Lewis acid, activating the hydroxyl group of the substrate for elimination.

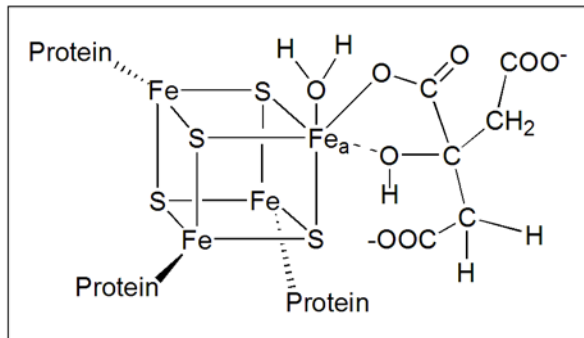


Figure 1-4: Substrate binding to iron-sulfur cluster of aconitase

1.2.b Dihydroxy-acid Dehydratase

Dihydroxy-acid dehydratase is involved in the biosynthesis of branched-chain amino acids and coenzyme A, and catalyzes the reaction shown in Figure 1-5. Characterization of *E. coli* dihydroxy-acid dehydratase by UV-visible, EPR, magnetic circular dichroism, and resonance Raman spectroscopies indicates that the enzyme

contains a $[4\text{Fe-4S}]^{2+,+}$ cluster with one non-cysteinyll coordinated iron site, similar to that seen in aconitase [16]. This suggests a role for the cluster in which the 3-hydroxyl group of the substrate could coordinate the Fe_a site of the cluster, and be activated for elimination. The enzyme is inactivated by oxidative degradation of the cluster, and in contrast to aconitase, cannot be reactivated with Fe^{2+} and thiol reducing agents.

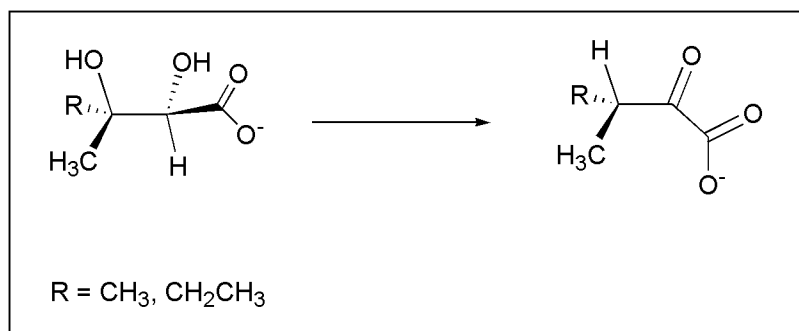


Figure 1-5: Reaction catalyzed by dihydroxy-acid dehydratase

1.2.c Serine Dehydratase

Two classes of enzymes are able to deaminate L-serine, producing pyruvate and ammonia. The mechanism involves generation of an enamine species, which is hydrolyzed to produce the final products of the reaction, as shown in Figure 1-6. The serine/threonine dehydratases have been fairly well characterized, and shown to utilize the cofactor pyridoxal 5'-phosphate in removal of the L-serine α -proton, allowing for β -elimination of the hydroxyl group. In contrast, the second class, the bacterial L-serine deaminases, have only been studied more recently. When purified anaerobically, reconstituted with iron and sulfide, and characterized by UV-visible, EPR, and Mössbauer spectroscopy, *E. coli* L-serine deaminase was found to contain one $[4\text{Fe-4S}]^{2+}$ cluster per polypeptide [17]. It is proposed that the cluster could serve a similar role as in

aconitase, with an Fe_a site coordinating the hydroxyl group of L-serine, and facilitating its elimination.

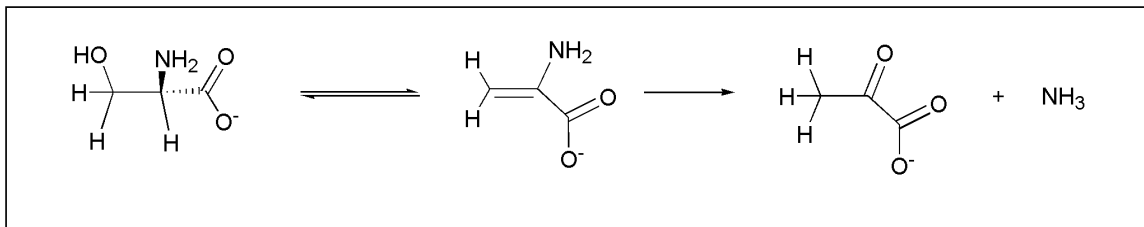


Figure 1-6: Deamination of L-serine

1.2.d Quinolinate Synthase

Quinolinate synthase is the enzyme responsible for formation of quinolinic acid, the common intermediate on the pathway to formation of NAD in both eukaryotes and prokaryotes. NadA performs the condensation reaction between iminoaspartate and dihydroxyacetone phosphate, generating quinolinic acid, inorganic phosphate, and 2 molecules of water (Figure 1-7). IA is generated *in vivo* by NadB, or chemically by reaction of OAA with ammonia [3]. An early study of NadB in the NadA/NadB system noted the lability of the NadA enzyme [18]. Further work suggested that NadA could be an iron-sulfur cluster containing enzyme, based on its decreased activity in the presence of hyperbaric oxygen, and the fact that it contained a CXXCXXC motif, which had been recognized in enzymes containing 4Fe-4S clusters, such as ferredoxin [7]. The first purification of *E. coli* NadA was from inclusion bodies produced upon overexpression of the protein [8]. The enzyme was reported to be active, although the methods for isolation from the inclusion bodies was not conducive for maintaining an iron-sulfur cluster, and no mention of an iron-sulfur cluster was made.

Recently, a combination of quantitative iron and sulfide analysis, in conjunction with UV-visible, Mössbauer, and EPR spectroscopy, showed that *E. coli* NadA contains a $[4\text{Fe-4S}]^{2+}$ cluster that is required for catalysis [9, 10]. Subsequently, the three cysteine residues that ligate the iron-sulfur cluster were identified in *E. coli*, suggesting a cluster similar to aconitase, in which there is an uncoordinated iron site to which a ligand can bind [19]. Surprisingly, the three cysteine residues involved in cluster ligation were not the three found in the CXXCXXC motif commonly associated with cluster ligation, but were those that appeared to be highly conserved across species [20, 21].

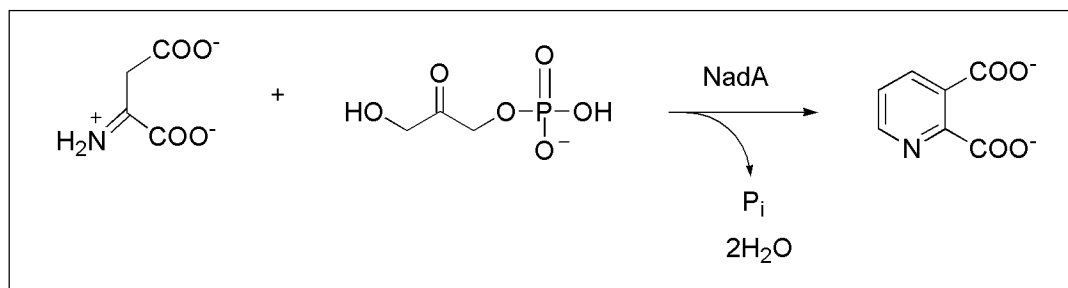


Figure 1-7: Reaction catalyzed by quinolinate synthase

1.3 Proposed Mechanisms of the Quinolinate Synthase Reaction

Although the exact mechanism of QA formation is not known, several have been suggested (Figure 1-8). In the mechanism proposed by Nasu *et al.* shown in Figure 1-6(a), C-C bond-formation with concomitant release of P_i occurs in the first step by attack of the C1 carbanion of IA onto C1 of DHAP [18]. The product then undergoes a keto-enol tautomerization followed by loss of a molecule of water upon Schiff base formation to close the ring. An additional molecule of water is eliminated in the final step of the

mechanism to generate the QA product. The mechanism set forth by Begley *et al.*, shown in Figure 1-6(b) differs significantly, beginning with an isomerization of DHAP to glyceraldehyde 3-phosphate (G3P) before the condensation reaction occurs. Schiff base formation between IA and G3P causes release of the first molecule of water, and is followed by intramolecular elimination of P_i [22]. The second molecule of water is eliminated in a dehydration step subsequent to pericyclic ring closure. Finally, Figure 1-6(c) shows a third mechanism, proposed by Booker, which combines aspects of both the Nasu and Begley mechanisms [23]. In the initial steps, P_i is released from G3P via an E1cb elimination, affording an α,β -unsaturated aldehyde, which reacts with the C3 carbanion of IA to form the C-C bond. A subsequent keto-enol tautomerization allows for Schiff-base formation, generating the first molecule of water and closing the ring. Dehydration of the resulting species affords the QA product. Regardless of the initial steps in the three proposed pathways, the final step requires that a hydroxyl group be removed from the precursor to quinolinic acid, which could be facilitated by the iron-sulfur cluster acting as a Lewis acid, withdrawing electron density so that the hydroxyl group can be eliminated. Although this role is identical to that of aconitase, the geometry of the quinolinic acid precursor would not allow for coordination to the Fe_a site through both hydroxyl and carboxyl groups. In the case of NadA, it is predicted that coordination to the cluster would be through the hydroxyl group alone, giving the Fe_a site four ligands (Figure 1-9). This is in contrast to other 4Fe-4S cluster enzymes, such as aconitase and the radical SAM enzymes, which have coordination numbers to the Fe_a site of 6 and 5, respectively. The monodentate manner of binding through the hydroxyl group

to be eliminated may also be seen in other iron-sulfur cluster hydro-lyases, such as L-serine deaminase [17].

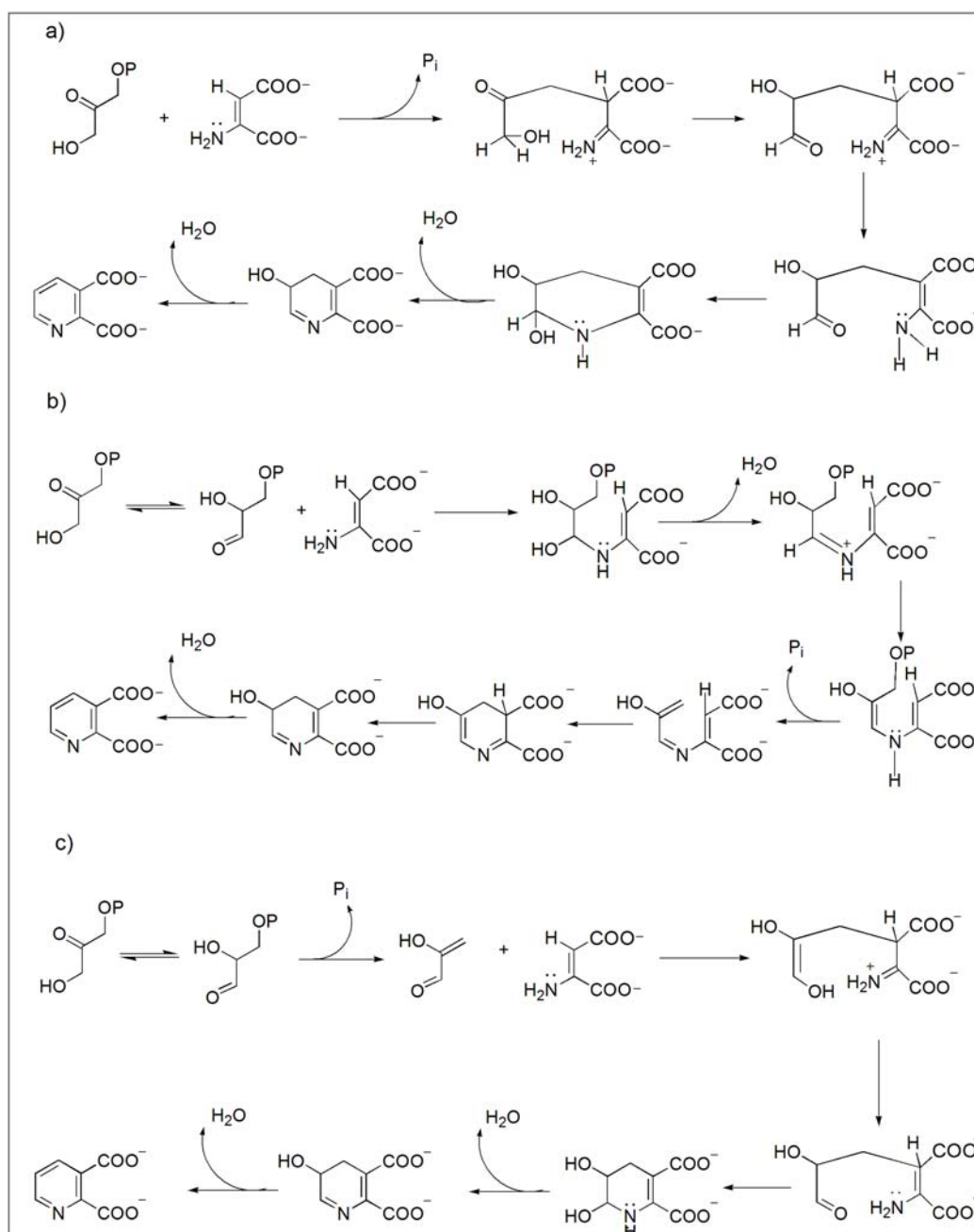


Figure 1-8: Proposed mechanisms of quinolinic acid formation as described by (a) Nasu et al¹⁸ (b) Begley et al²² and (c) Booker²³

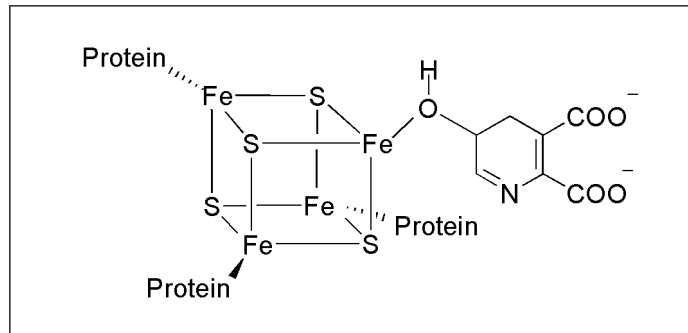


Figure 1-9: Proposed mode of quinolinic acid precursor binding to cluster

1.4 Crystal Structure of Quinolinate Synthase

While structures of NadB from several different organisms have been published, [5, 24] only one structure of NadA has been produced. A genomic approach was used to identify the NadA gene in the hyperthermophilic archaeon *Pyrococcus horikoshii* [25]. Subsequently, the NadA protein was purified, catalytic activity was reported, and the protein was crystallized. However, the protein structure did not contain an iron-sulfur cluster, nor was there mention of a cluster in the paper. In addition, there were three surface loops on the protein that were unable to be defined because of a lack of electron density, each containing one of the cysteine residues analogous to those ligating the cluster in *E. coli* NadA. Therefore, purification under anaerobic conditions which should facilitate stabilization of the Fe/S cluster, may constrain the mobility of the surface loops and allow for better resolution of the protein in the active site area. A detailed picture of this region should also help answer mechanistic questions, such as the order of DHAP and IA binding, whether the phosphate group is lost from DHAP before the condensation

begins, and whether the QA precursor binds the cluster through its hydroxyl group, as predicted.

1.5 Specific Aims

In an effort to show the essential nature of the 4Fe-4S cluster in quinolinate synthases, and begin to elucidate its role in catalysis, the following specific aims were investigated:

- (1) Purification and characterization of *E. coli* NadA apoprotein, lacking the iron-sulfur cluster.
- (2) Purification and characterization of wild-type and variant NadA from *Mycobacterium tuberculosis*.
- (3) Cloning, purification, characterization and crystallization of *P. horikoshii* NadA.

1.6 References

1. Belenky, P., Bogan, K. L., and Brenner, C. (2007) NAD⁺ metabolism in health and disease. *Trends Biochem. Sci.* 32, 12-19.
2. Pollack, N., Dölle, C., and Ziegler, M. (2007) The power to reduce: pyridine nucleotides-small molecules with a multitude of functions. *Biochem. J.* 402, 205-218.
3. Nasu, S., and Gholson, R. K. (1981) Replacement of the B protein requirement of the *E. coli* quinolinate synthetase system by chemically-generated iminoaspartate. *Biochem. Biophys. Res. Commun.* 101, 533-539.

4. Mortarino, M., Negri, A., Tedeschi, G., Simonic, T., Duga, S., Gassen, H. G., and Ronchi, S. (1996) L-Aspartate oxidase from *Escherichia coli*. I. Characterization of coenzyme binding and product inhibition. *Eur. J. Biochem.* 239, 418-426.
5. Bossi, R., Negri, A., Tedeschi, G., and Mattevi, A. (2002) Structure of FAD-bound L-aspartate oxidase: insight into substrate specificity and catalysis. *Biochemistry* 41, 3018-3024.
6. Draczynska-Lusiak, B., and Brown, O.R. (1992) Protein A of quinolinate synthetase is the site of oxygen poisoning of pyridine nucleotide coenzyme synthesis in *Escherichia coli*. *Free Radical Biol. Med.* 13, 689-693.
7. Gardner, P. R., and Fridovich, I. (1991) Quinolinate synthetase: The oxygen-sensitive site of de novo NAD(P)⁺ biosynthesis. *Arch. Biochem. Biophys.* 284, 106-111.
8. Cecilian, F., Caramori, T., Ronchi, S., Tedeschi, G., Mortarino, M., and Galizzi, A. (2000) Cloning, overexpression, and purification of *Escherichia coli* quinolinate synthetase. *Prot. Express. Purif.* 18, 64-70.
9. Cicchillo, R. M., Tu, L., Stromberg, J. A., Hoffart, L. M., Krebs, C., and Booker, S. J. (2005) *Escherichia coli* quinolinate synthetase does indeed harbor a [4Fe-4S] cluster. *J. Am. Chem. Soc.* 127, 7310-7311.
10. Ollagnier-de Choudens, S., Loiseau, L., Sanakis, Y., Barras, F., and Fontecave, M. (2005) Quinolinate synthetase, an iron-sulfur enzyme in NAD biosynthesis. *FEBS Lett.* 579, 3737-3743.
11. Flint, D. H., and Allen, R. M. (1996) Iron-sulfur proteins with nonredox functions. *Chem Rev* 96, 2315-2234.

12. Beinert, H., and Kennedy, M. C. (1993) Aconitase, a two-faced protein: enzyme and iron regulatory factor. *FASEB J.* 7: 1442-1449.
13. Dickman, S. R., and Cloutier, A. A. (1951) Factors affecting the activity of aconitase. *J. Biol. Chem.* 188, 379-388.
14. Lauble, H., Kennedy, M.C., Beinert, H., and Stout, C. D. (1992) Crystal structures of aconitase with isocitrate and nitrocitrate bound. *Biochemistry* 31, 2735-2748.
15. Lauble, H., Kennedy, M.C., Beinert, H., Stout, D.C. (1994) Crystal structures of aconitase with *trans*-aconitate and nitrocitrate bound. *J. Mol. Biol.* 23, 437-451.
16. Flint, D. H., Emptage, M. H., Finnegan, M. G., Fu, W., and Johnson, M. K. (1993) The role and properties of the iron-sulfur cluster in *Escherichia coli* dihydroxy-acid dehydratase. *J. Biol. Chem.*, 268, 14732-14742.
17. Cicchillo, R. M., Baker, M. A., Schnitzer, E. J., Newman, E. B., Krebs, C., and Booker, S. J. (2004) *Escherichia coli* L-serine deaminase requires a [4Fe-4S] cluster in catalysis. *J. Biol. Chem.* 279, 32418-32425.
18. Nasu, S., Wicks, F. D., and Gholson, R. K. (1982) L-aspartate oxidase, a newly discovered enzyme of *Escherichia coli*, is the B protein of quinolinate synthetase. *J. Biol. Chem.* 257, 626-632.
19. Saunders, A. H., Griffiths, A. E., Lee, K., Cicchillo, R. M., Tu, L., Stromberg, J. A., Krebs, C., and Booker, S. J. (2008) Characterization of quinolinate synthases from *Escherichia coli*, *Mycobacterium tuberculosis*, and *Pyrococcus horikoshii* indicates that [4Fe-4S] clusters are common cofactors throughout this class of enzymes. *Biochemistry, Submitted.*

20. The_UniProt_Consortium. (2007) The Universal Protein Resource (UniProt). *Nucleic Acids. Res.* 35, D193-197.
21. Murthy, U. M., N., Ollagnier-de-Choudens, S., Sanakis, Y., Abdel-Ghany, S. E., Rousset, C., Ye, H., Fontecave, M., Pilon-Smits, E. A. H., and Pilon, M. (2007) Characterization of *Arabidopsis thaliana* SufE2 and SufE3: Functions in chloroplast iron-sulfur cluster assembly and NAD synthesis. *J. Biol. Chem.* 282, 18254-18264.19.
22. Begley, T., Kinsland, C., Mehl, R., Osterman, A., Dorrestein, P. (2001) The biosynthesis of nicotinamide adenine dinucleotides in bacteria. *Vitam. Horm.* 61, 103-119.
23. Booker, S. J. personal communication.
24. Sakuraba, H., Yoneda, K., Asai, I., Tsuge, H., Katunuma, N., and Ohshima, T. (2008) Structure of L-aspartate oxidase from the hyperthermophilic archaeon *Sulfolobus tokodaii*. *Biochim. Biophys. Acta* 1784, 563-571.
25. Sakuraba, H., Tsuge, H., Yoneda, K., Katunuma, N., and Ohshima, T. (2005) Crystal structure of the NAD biosynthetic enzyme quinolinate synthase. *J. Biol. Chem.* 280, 26645-26648.

Chapter 2:

The *Escherichia coli* Quinolinate Synthase [4Fe-4S] Cluster Is Required for Catalysis

2.1 Introduction

Quinolinate synthase (NadA) is the enzyme responsible for the formation of QA, a key intermediate in both the prokaryotic and eukaryotic pathways for synthesis of the cofactor nicotinamide adenine dinucleotide (NAD). NadA catalyzes the condensation reaction between iminoaspartate and dihydroxyacetone phosphate (DHAP), forming quinolinic acid. Initially, the presence of an Fe/S cluster in NadA was hypothesized based on observed oxygen sensitivity of the protein and the presence of a CXXCXXC motif known to ligate such clusters [1]. More recently, work by both the Booker and Fontecave groups found that *E. coli* NadA contains one $[4\text{Fe-4S}]^{2+}$ cluster per protein [2, 3]. This places quinolinate synthase in the class of hydro-lyases that contain Fe/S clusters, including many that utilize the cluster in catalysis [4].

In their paper describing the Fe/S cluster in NadA, the Fontecave group reported that the cluster is absolutely required for catalysis, based on experiments showing that DHAP is not consumed in an assay containing an apo form of NadA. The apo form was obtained by aerobic purification of the enzyme, and supported by the pink color of the as-isolated (AI) protein and substoichiometric amounts of iron and sulfide [3]. Work done by the Booker group found that isolated protein from *E. coli* did not appear to be as oxygen-sensitive as had been reported earlier. Both groups drew the parallel between the NadA enzyme and aconitase, another member of the Fe/S-dependent hydrolyases.

Aconitase has been studied in detail and requires the [4Fe-4S] cluster for catalysis, utilizing it as a Lewis acid to facilitate dehydration of the substrate [5, 6]. It therefore appears that the cluster in NadA could serve a similar role, catalyzing the elimination of a hydroxyl group as a molecule of water from one of the intermediates formed during the reaction.

The first crystal structure of NadA was published in 2005, and called into question the essential nature of the cluster. The structure did not show an Fe/S cluster at the active site of the protein, nor was there mention of cluster involvement in catalysis, although activity was reported for the crystallized protein [7]. In the work described here, NadA apoprotein is produced by chelating iron from the media during protein expression [8]. The isolated apoprotein is then characterized by UV-visible and electron paramagnetic resonance (EPR) spectroscopy, in addition to iron and sulfide quantification. Activity analysis confirms that the cluster-less protein does not have quinolinate synthase activity. In addition, it was found that the cluster could be chemically reconstituted, restoring the activity of the protein.

2.2 Materials and Methods

Materials

All DNA modifying enzymes and reagents were purchased from New England Biolabs (Beverly, MA). PfuUltraTM High Fidelity DNA Polymerase and its associated 10× reaction buffer were obtained from Stratagene (La Jolla, CA). Oligonucleotide primers for cloning were obtained from Integrated DNA Technologies (Carlsbad, CA). *Escherichia coli* genomic DNA (strain W3110) was obtained from Sigma Corp (St. Louis, MO). Coomassie blue dye-binding reagent for protein concentration

determination and the bovine serum albumin (BSA) standard (2 mg mL⁻¹) were obtained from Pierce (Rockford, IL). Nickel nitrilotriacetic acid (Ni-NTA) resin was purchased from Qiagen (Valencia, CA). Sephadex G-25 resin and PD-10, NICK and NAP pre-poured gel filtration columns were purchased from GE Biosciences (Piscataway, NJ). 2,3-Pyridinedicarboxylic acid (QA standard) was obtained from Aldrich (St. Louis, MO). Dihydroxyacetone phosphate (dilithium salt) was obtained from Sigma (St. Louis, MO), and *o*-phenanthroline was obtained from Fisher (Fair Lawn, NJ). All other buffers and chemicals were of the highest grade available.

General Procedures

High performance liquid chromatography (HPLC) was conducted on a Beckman System Gold unit (Fullerton, CA), which was fitted with a 128 diode array detector and operated with the System Gold *Nouveau* software package. Iron and sulfide analysis was performed as previously described [9-11]. Sonic disruption of *E. coli* cells was carried out with a 550 sonic dismembrator from Fisher Scientific (Pittsburgh, PA) in combination with a horn containing a ½ in. tip.

Spectroscopic Methods

UV-visible spectra were obtained on a Cary 50 spectrometer (Varian; Walnut Creek, CA) using the associated WinUV software package. Low-temperature X-band EPR spectroscopy was carried out in perpendicular mode on a Bruker (Billerica, MA) ESP 300 spectrometer equipped with an ER 041 MR microwave bridge and an ST4102 X-band resonator (Bruker). The sample temperature was maintained with an ITC503S temperature controller and an ESR900 liquid helium cryostat (Oxford Instruments; Concord, MA).

Cloning of Escherichia coli NadA and NadB

The *nadA* gene was cloned by PCR into a pET28a expression vector, which is isopropyl- β -D-thiogalactopyranoside (IPTG)-inducible, such that the protein contains an N-terminal hexahistidine tag. The *nadA* gene was amplified from *E. coli* (strain W3110) genomic DNA by PCR using the forward primer, 5'-GCG-GCG-TCC-ATA-TGA-GCG-TAA-TGT-TTG-ATC-CAG-ACA-CGG-CG-3', containing a *NdeI* restriction site and reverse primer, 5'-GCC-GGA-ATT-CTT-ATC-CAC-GTA-GTG-TAG-CCG-CAA-AAT-CCA-GC-3', containing an *EcoRI* restriction site (restriction sites underlined). Each amplification reaction contained the following in a volume of 50 μ L: 0.4 μ M of each primer, 0.2 mM of each deoxynucleoside triphosphate, 100 ng of *E. coli* genomic DNA, 2.5 U of PfuUltraTM High Fidelity DNA Polymerase, and 5 μ L of 10 \times PfuUltraTM reaction buffer. The reaction mixture was overlaid with 30 μ L of mineral oil. After a 2 min denaturation step at 95 $^{\circ}$ C, 30 cycles of the following program were initiated: 30 sec at 95 $^{\circ}$ C, 30 sec at 70 $^{\circ}$ C, 1 min at 72 $^{\circ}$ C. The reaction was finalized at 72 $^{\circ}$ C for 10 min. The PCR product was digested with *NdeI* and *EcoRI* and then ligated into a pET28a expression vector digested with the same enzymes. The *nadB* gene was amplified from *E. coli* (strain W3110) genomic DNA by PCR using the forward primer, 5'-GCG-GCG-TCC-ATA-TGA-ATA-CTC-TCC-CTG-AAC-ATT-CAT-GTG-ACG-TGT-TGA-TTA-TCG-G-3', containing a *NdeI* restriction site, and reverse primer, 5'-GCG-CGA-AGC-TTT-TAT-CTG-TTT-ATG-TAA-TGA-TTG-CCG-GGG-GAA-AGG-ATC-GAC-GG-3', containing a *HindIII* restriction site (enzyme restriction sites underlined). Each amplification reaction contained the same concentrations of materials above for amplification of the *nadA* gene in addition to 4% DMSO. After a 2 min denaturation step

at 95 °C, 30 cycles of the following program were initiated: 30 sec at 95 °C, 30 sec at 63 °C, 3 min at 72 °C. The reaction was finalized at 72 °C for 10 min. The PCR product was digested with *NdeI* and *HindIII* and then ligated into a pET28a expression vector digested with the same enzymes. All other procedures were carried out by standard methods. DNA sequencing was carried out at the Pennsylvania State University Nucleic Acid Facility.

Expression of E. coli NadA Apoprotein

A single colony was used to inoculate 100 mL of Luria–Bertani (LB) media containing 50 µg/mL kanamycin and 100 µg/mL ampicillin and was grown for approximately 7 h at 37 °C with shaking. A 60 mL portion of the culture was then evenly distributed among four 6 L Erlenmeyer flasks to inoculate 16 L of LB media containing 50 µg/mL kanamycin and 100 µg/mL ampicillin, and was cultured further at 37 °C with shaking (180 rpm). At an OD₆₀₀ of 0.6, 100 mM *o*-phenanthroline in 100 mM HCl was added to a final concentration of 100 µM. The cultures were then incubated for 15 min before induction with IPTG to a final concentration of 200 µM. Following induction, the cultures were grown for 4 h at 37 °C with shaking (180 rpm). Cells were harvested at 10,000 × *g* for 10 min at 4 °C, and the cell paste was frozen in liquid N₂ and stored at -80 °C until ready for use.

Purification of E. coli NadA Apoprotein

All steps of the purification were carried out inside of an anaerobic chamber from Coy Laboratory Products, Inc. (Grass Lake, MI) under an atmosphere of N₂ and H₂ (95%/5%) with an O₂ concentration maintained below 1 ppm by the use of palladium

catalysts. Steps using centrifugation were performed outside of the anaerobic chamber in centrifuge tubes that were tightly sealed before removal from the chamber. All buffers were prepared using distilled and deionized water that was boiled for at least 1 h and then allowed to cool uncapped with stirring in the anaerobic chamber for 48 h. All plastic ware was autoclaved and brought into the chamber hot and allowed to equilibrate overnight before use.

Protein purification was carried out by immobilized metal affinity chromatography using a nickel-nitrilotriacetic acid (Ni-NTA) matrix. In a typical purification, 25 g of frozen cells were resuspended in 80 mL of buffer A (50 mM HEPES, pH 7.5, 0.3 M KCl, 20 mM imidazole, and 10 mM 2-mercaptoethanol). Solid egg white lysozyme was added to a final concentration of 1 mg mL⁻¹ and the mixture was stirred at room temperature for 30 min. After the cells were cooled in an ice-water bath to <8 °C, the cells were subjected to four 1 min bursts of sonic disruption (setting 7). The cellular debris was removed by centrifugation at 50,000 × *g* for 1 h, and the supernatant was loaded onto a Ni-NTA column (2.5 x 7 cm) equilibrated in buffer A. The column was washed with 100 mL of buffer B (50 mM HEPES, pH 7.5, 0.3 M KCl, 40 mM imidazole, 10 mM 2-mercaptoethanol, and 20% glycerol) and subsequently eluted with buffer B containing 250 mM imidazole. Fractions that were brown in color were pooled and concentrated in an Amicon stirred cell (Millipore, Billerica, MA) fitted with a YM-10 membrane (10,000 Da MW cutoff). The protein was exchanged into buffer C (50 mM HEPES, pH 7.5, 0.1 M KCl, 10 mM DTT, and 20% glycerol) by anaerobic gel filtration (Sephadex G-25), concentrated and stored in aliquots in a liquid N₂ dewar until ready for use, or immediately reconstituted (see below) with iron and sulfide. All buffers were

chilled on ice prior to use and ice packs were used during protein concentration steps to keep the protein cold.

Reconstitution of NadA

Reconstitution of NadA with iron and sulfide was carried out on ice in a Coy anaerobic chamber using anaerobic buffers and solutions. A typical reconstitution contained, in a final volume of 20 mL, 100 μ M NadA that was initially treated with 5 mM DTT for 20 min. Then an 8-fold molar excess of FeCl₃ was added and the solution was allowed to sit on ice for 20 min. Finally, an 8-fold molar excess of Na₂S was added over the period of 3 to 4 h, followed by incubation on ice for at least 5 h to a maximum of 13h (overnight). The solution was then concentrated in an Amicon stirred cell, placed in airtight centrifuge tubes, removed from the anaerobic chamber, and centrifuged at 14,000 $\times g$ for 2 min to remove precipitate. The reconstituted (RCN) samples were brought back into the anaerobic chamber, and the supernatants were removed and exchanged into buffer C by gel filtration (Sephadex G-25 or Amersham PD-10), and then reconcentrated and stored in aliquots in a liquid N₂ dewar.

Purification of E. coli NadB

A single colony was used to inoculate 100 mL of Luria–Bertani (LB) media containing 50 μ g/mL kanamycin, and was grown for 7 h at 37 °C with shaking. A 60 mL portion of the culture was evenly distributed to four 6 L Erlenmeyer flasks to inoculate 16 L of LB media containing 50 μ g/mL kanamycin, and was cultured further at 37 °C. At an OD₆₀₀ of 0.6, the cultures were cooled in an ice-water bath and solid IPTG and FAD were added to each flask to final concentrations of 200 and 10 μ M, respectively. The cultures

were then incubated at 18 °C with shaking for 16 h. Cells were harvested at $10,000 \times g$ for 10 min at 4 °C, affording typical yields of 50-60 g of cell paste, which was frozen in liquid N₂ and stored at -80 °C until ready for use.

In a typical purification, 25 g of frozen cells were resuspended in 80 mL of buffer D (50 mM HEPES, pH 7.5, 0.2 M NaCl, 10 mM imidazole, 10 mM succinate, pH 8, and 20 µM FAD). Solid egg white lysozyme and phenylmethanesulfonyl fluoride (PMSF) were added to final concentrations of 1 mg mL⁻¹ and 1 mM, respectively, and the mixture was stirred at room temperature for 30 min. After the solution was cooled in an ice-water bath to <8 °C, it was subjected to four 1 min bursts of sonic disruption (setting 7). Cellular debris was removed by centrifugation at $50,000 \times g$ for 1 h and the supernatant was loaded onto a Ni-NTA column (2.5 x 7 cm) equilibrated in buffer D. The column was washed with 175 ml of buffer E (50 mM HEPES, pH 7.5, 0.2 M NaCl, 20 mM imidazole, 10 mM succinate, pH 8, 20 µM FAD, and 10% glycerol) and subsequently eluted with buffer E containing 250 mM imidazole. Protein-containing fractions were pooled and concentrated in an Amicon stirred cell (Millipore, Billerica, MA) fitted with a YM-10 membrane (10,000 Da MW cutoff). The protein was exchanged into anaerobic buffer F (50 mM HEPES, pH 7.5, and 10% glycerol) by anaerobic gel filtration (Sephadex G-25), reconcentrated, and stored in aliquots in a liquid N₂ dewar until ready for use.

Determination of Protein Concentration

Protein concentrations were determined by the Bradford dye staining procedure with BSA as the standard [12]. Parallel samples were subjected to quantitative amino

acid analysis at the University of Iowa's Molecular Analysis Facility to confirm that the Bradford assay was accurate without a correction factor.

Assay for Quinolinic Acid

The activity of *E. coli* NadA was determined by monitoring the formation of QA over a twenty-minute time period at 37 °C under anaerobic conditions. The substrate IA was generated enzymatically from L-aspartate by NadB using fumarate as the electron acceptor. The assay contained, in a final volume of 1300 µL, 200 mM HEPES, pH 7.5, 25 mM L-aspartate/fumarate solution, pH 7, 25 µM FAD, 1 mM DHAP, 0.1 M KCl, 0.3 mM L-tryptophan (internal standard), and 15 µM NadA and 15 µM NadB. The reactions were initiated by addition of NadB after incubation of the other components in the assay mixture at 37 °C for 5 min. At designated times, 200 µL aliquots of the assay mixture were removed and added to 40 µL of 2 M trichloroacetic acid to quench the reaction. The precipitated protein was pelleted by centrifugation and the supernatant was analyzed by HPLC with UV detection (268 nm) using a Zorbax SB-C18 column (4.6 x 250 mm), which was obtained from Agilent. The column was equilibrated in 100% Solvent A (1% TFA) at a flow rate of 1 mL min⁻¹. These initial conditions were maintained for 10 min after injection, after which a gradient of 0-45% Solvent B (acetonitrile) was applied over 10 min. At 20 min, a gradient of 45-90% Solvent B was applied over 3 min. Finally, at 25 min, a gradient of 90-0% Solvent B was applied over 3 min to re-establish the initial conditions until the end of the run at 32 min. Using this method, QA eluted at 8.3 min and the tryptophan internal standard eluted at 20.3 min. The concentration of QA was

determined from a calibration curve of known concentrations of QA, using the internal standard to correct for volume changes between sample injections.

Preparation of EPR Samples

Samples to be analyzed by EPR spectroscopy were prepared inside of the anaerobic chamber, and contained ~300 μ M NadA in a total volume of 250 μ L. Reduced samples were treated with 2 mM sodium dithionite at room temperature for approximately 5 min before loading into EPR tubes (2 mm i.d.) and freezing in liquid nitrogen.

2.3 Results

*Expression of *E. coli* NadA Apoprotein*

E. coli NadA in a cluster-free apo form was generated by expression of the *nadA* gene in the presence of 100 μ M *o*-phenanthroline in the growth media, a method that had previously been employed to generate an apo form of the R2 subunit of *E. coli* ribonucleotide reductase containing a Phe208Tyr substitution [8]. LB media contains approximately 17 μ M iron [13]. Addition of the iron chelator to the media shortly before induction of the protein appeared to sequester the available iron, preventing its incorporation into the protein. Following induction, the cells were incubated for 4 h at 37° C with shaking before harvesting by centrifugation. Production of the protein, as observed by SDS-PAGE (Figure 2-1), was similar to that previously seen for the *E. coli* NadA holoprotein, although the yield of cell paste (2 g/L) after 4 h was less than the ~3.5g/L typically obtained in the absence of *o*-phenanthroline addition. The resulting cell paste was light tan in color, in contrast to the dark brown cell paste typically obtained with the holoprotein.

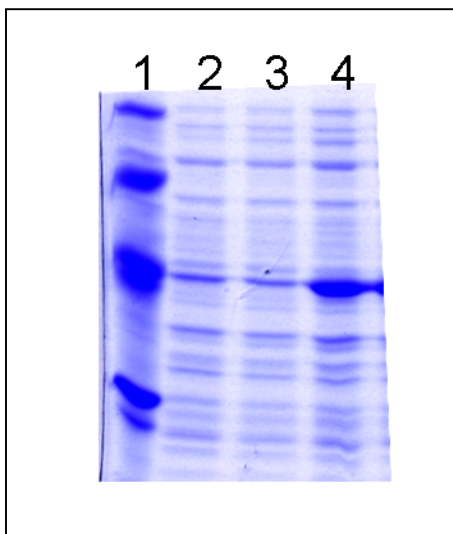


Figure 2-1: SDS-PAGE of *E. coli* NadA apoprotein expression

Lane 1: molecular weight standards, 97.0, 66.0, 45.0, 30.0 kDa from top; Lane 2: at addition of 100 μ M *o*-phenanthroline; Lane 3: at induction with 200 μ M IPTG; Lane 4: 1 hour after induction with IPTG

Purification and Characterization of E. coli NadA Apoprotein

E. coli NadA apoprotein was purified in the same manner as previously described for NadA containing an Fe/S cluster [2]. The use of an N-terminal hexahistidine tag allowed specific purification in one step, affording a pure product (Figure 2-2, lane 6). Typical protein yields were 3-5 mg per gram of cell paste. The protein was nearly colorless, and its UV-visible spectrum was silent beyond 300 nm, in contrast to that displayed by holo-NadA, which typically includes a shoulder around 320 nm, a peak around 400 nm, and broad tailing that extends beyond 700 nm (Figure 2-3, solid line). Upon chemical reconstitution of the protein with the reductant DTT and 8-fold excesses of ferric chloride and sodium sulfide, the cluster was regenerated, as demonstrated by the dark brown color of the protein - similar to that of as-isolated holoprotein - and the

corresponding increase in absorbance at 400 nm (Figure 2-3, dashed line). The absorbance ratio, A_{280}/A_{400} , for the reconstituted protein was ~ 2.7 , similar to that previously found for the reconstituted cluster-containing protein (unpublished results). Quantification of iron and sulfide indicated that the AI apoprotein contained 0.4 ± 0.3 irons per polypeptide, and sulfide that was below the limit of detection of the assay. After reconstitution, NadA contained 5.8 ± 0.4 irons and 5.0 ± 0.2 sulfides per protein, similar to those previously found for reconstituted holoprotein [2].

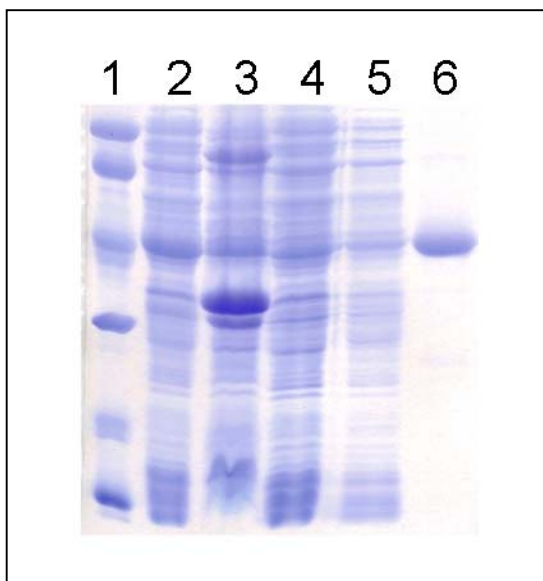


Figure 2-2: SDS-PAGE of *E. coli* NadA apoprotein purification

Lane 1: molecular weight standards, 97.0, 66.0, 45.0, 30.0, 20.1, 14.4 kDa from top; Lane 2: lysate supernatant; Lane 3: lysate pellet; Lane 4: Ni-NTA column load eluate; Lane 5: Ni-NTA column wash eluate; Lane 6: purified protein

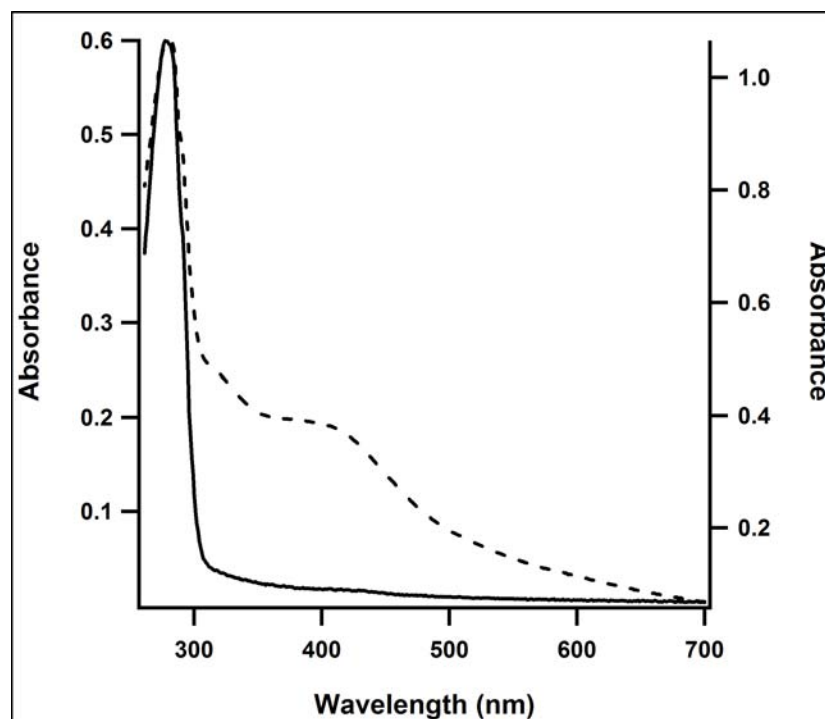


Figure 2-3: UV-visible spectra of AI (solid line, left axis) and RCN (dashed line, right axis) Apo-NadA from *E. coli*.

Activity Analysis

While the AI apoprotein did not exhibit quinolinate synthase activity, chemical reconstitution of the protein fully restored activity. Using 15 μM NadA apoprotein in the assay and enzymatically generated IA, no QA formation was observed, even after 20 min of incubation (Figure 2-4, black circles). When the reconstituted protein was assayed under the same conditions, it displayed a $V_{\text{max}}/[E_T]$ of 0.34 min^{-1} (Figure 2-4, red squares), nearly identical to the 0.30 min^{-1} previously observed for the AI holoprotein (unpublished results). In order to demonstrate that the restored activity of the holoprotein was due to the formation of an intact cluster, aliquots of the apoprotein were incubated with DTT alone, DTT and ferric chloride, or DTT and sodium sulfide according to the

reconstitution procedure described above. None of these proteins exhibited quinolinate synthase activity.

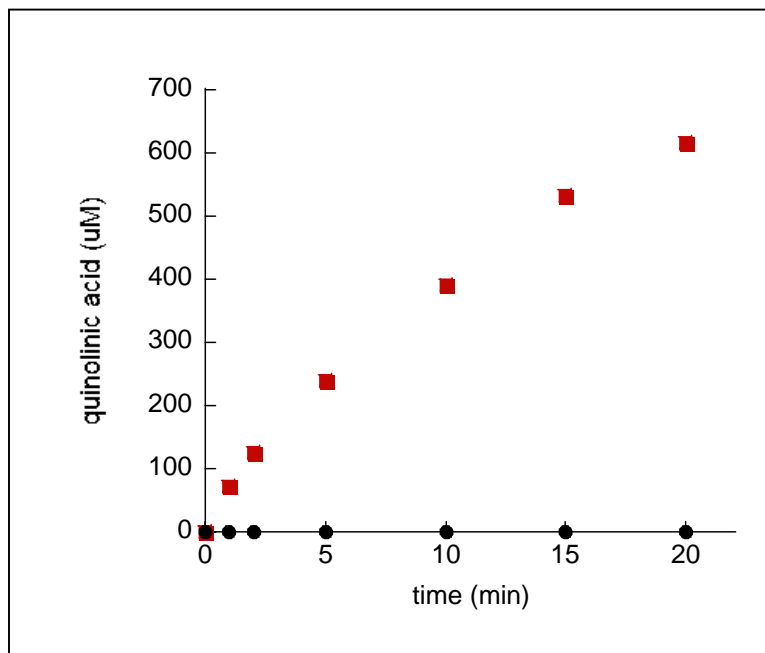


Figure 2-4: Activity assay of AI (black circles) and RCN (red squares) Apo-NadA from *E. coli*

EPR spectroscopy

EPR spectroscopy was used to confirm the presence of the $[4\text{Fe-4S}]^{2+}$ cluster in the reconstituted holoprotein. The EPR samples were prepared by incubating the AI apoprotein and the RCN holoprotein with 2 mM sodium dithionite before flash-freezing in EPR tubes. The spectrum generated at 13K and 5 mW power showed no signal for the reduced apoprotein, indicating that no paramagnetic species was present (Figure 2-5, solid line). However, the reduced RCN apoprotein did produce a rhombic signal with g values of 2.05, 1.93 and 1.87, nearly identical to those of the AI *E. coli* NadA holoprotein (Figure 2-5, dashed line) [2].

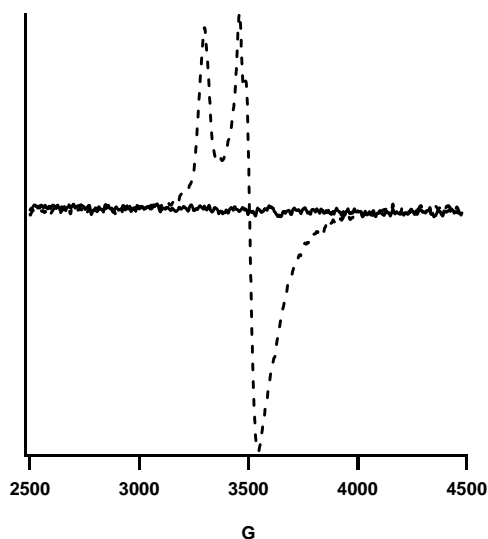


Figure 2-5: EPR spectra of AI (solid line) and RCN (dashed line) Apo-NadA from *E. coli*.

2.4 Discussion

The addition of the metal chelator, *o*-phenanthroline, to the growth medium during NadA expression successfully sequestered iron from the medium, so that the protein was expressed in its apo form. Previous efforts by our lab to produce apo-NadA from isolated holoprotein using the methods of the Marquet [14] and Beinert groups [15] did not remove significant amounts of cluster from the protein. In addition, the cluster did not appear to be as sensitive to oxidative degradation as had previously been indicated [1]. Therefore, the *o*-phenanthroline method, previously used to obtain ribonucleotide reductase lacking its dinuclear iron cluster, was utilized [8]. Without any other alterations to the procedures used to produce and purify holoprotein, apoprotein was isolated in amounts sufficient for study. As expected, apo-NadA was nearly colorless in appearance, contained negligible amounts of iron and sulfide, and lacked quinolinate synthase activity.

Isolated apo NadA was easily converted to its active cluster-containing form by chemical reconstitution, demonstrating that the addition of *o*-phenanthroline to the growth medium did not have any adverse effects on the normal formation of the protein. The apoprotein was incubated on ice overnight with excess reductant, iron, and sulfide, and then subjected to gel filtration to remove any unbound iron and sulfide. The resulting protein had characteristics similar to AI holoprotein – a brown color and broad UV-visible absorbance around 400 nm, and amounts of iron and sulfide consistent with the presence of one [4Fe-4S] cluster per protein. EPR spectroscopy of the reduced apoprotein showed no signal, while the spectrum generated by the reduced RCN protein was nearly identical to that previously found for the reduced AI holoprotein [2].

While the spectroscopic evidence and iron and sulfide quantification show that the [4Fe-4S] can be successfully added back in to the apoprotein, the results of the activity assay definitively demonstrate that this cluster is essential for catalysis. The RCN protein has an activity of 0.34 min^{-1} , nearly identical to that of AI holoprotein. To confirm that the restored activity is a result of cluster restoration, and not merely from the incubation with reductant, the originally isolated apoprotein was also submitted to several “mock” reconstitution procedures, in which it was incubated overnight with DTT alone, DTT and the iron source, or DTT and the sulfide source. In all of these cases, the resulting protein lacked any quinolinate synthase activity. Thus it was demonstrated that the [4Fe-4S] cluster in *E. coli* quinolinate synthase is essential for catalysis.

2.5 References

1. Gardner, P. R., and Fridovich, I. (1991) Quinolinate synthetase: The oxygen-sensitive site of de novo NAD(P)⁺ biosynthesis. *Arch. Biochem. Biophys.* 284, 106-111.
2. Cicchillo, R. M., Tu, L., Stromberg, J. A., Hoffart, L. M., Krebs, C., and Booker, S. J. (2005) *Escherichia coli* quinolinate synthetase does indeed harbor a [4Fe-4S] cluster. *J. Am. Chem. Soc.* 127, 7310-7311.
3. Ollagnier-de Choudens, S., Loiseau, L., Sanakis, Y., Barras, F., and Fontecave, M. (2005) Quinolinate synthetase, an iron-sulfur enzyme in NAD biosynthesis. *FEBS Lett.* 579, 3737-3743.
4. Flint, D. H., and Allen, R. M. (1996) Iron-sulfur proteins with nonredox functions. *Chem Rev* 96, 2315-2234.
5. Emptage, M. H., Dreyer, J. L., Kennedy, M. C., and Beinert, H. (1983) Optical and EPR characterization of different species of active and inactive aconitase. *J. Biol. Chem.* 258, 11106-11111.
6. Emptage, M. H., Kent, T. A., Kennedy, M. C., Beinert, H., and Münck, E. (1983) Mössbauer and EPR studies of activated aconitase: Development of a localized valence state at a subsite of the [4Fe-4S] cluster on binding of citrate. *Proc. Natl. Acad. Sci. USA* 80, 4674-4678.
7. Sakuraba, H., Tsuge, H., Yoneda, K., Katunuma, N., and Ohshima, T. (2005) Crystal structure of the NAD biosynthetic enzyme quinolinate synthase. *J. Biol. Chem.* 280, 26645-26648.

8. Parkin, S. E., Chen, S., Ley, B. A., Mangravite, L., Edmondson, D. E., Huynh, B. H., and Bollinger, J. M., Jr., (1998) Electron injection through a specific pathway determines the outcome of oxygen activation at the diiron cluster in the F208Y mutant of *Escherichia coli* ribonucleotide reductase. *Biochemistry* 37, 124-1130.
9. Beinert, H. (1978) Micro methods for the quantitative determination of iron and copper in biological material. *Methods Enzymol* 5, 435-445.
10. Beinert, H. (1983) Semi-micro methods for analysis of labile sulfide and of labile sulfide plus sulfane sulfur in unusually stable iron-sulfur proteins. *Anal. Biochem.* 131, 373-378.
11. Kennedy, M.C., Kent, T. A., Emptage, M., Merkle, H., Beinert, H., and Münck, E. (1984) Evidence for the formation of a linear [3Fe-4S] cluster in partially unfolded aconitase. *J. Biol. Chem.* 259, 14463-14471.
12. Bradford, M. M. (1976) A rapid and sensitive method for the quantitation of microgram quantities of protein utilizing the principle of protein-dye binding. *Anal. Biochem.* 72, 248 - 254.
13. Yang, Y., Harris, D. P., Luo, F., Wu, L., Parsons, A. B., Palumbo, A. V., and Zhou, J. (2008) Characterization of the *Shewanella oneidensis* Fur gene: roles in iron and acid tolerance response. *BMC Genomics* 9, S1-11.
14. Lotierzo, M., Raux, E., Bui B., T. S., Goasdoue, N., Libot F., Florentin, D., Warren, M. J., and Marquet, A. (2006) Biotin synthase mechanism: mutagenesis of the YNHNLD conserved motif. *Biochemistry* 45, 12274-12281.

15. Kennedy, M. C. , and Beinert, H. (1988) The state of cluster SH and S²⁻ of aconitase during cluster interconversions and removal: A convenient preparation of apoenzyme. *J. Biol. Chem.* 263, 8194-819.

Chapter 3:

Purification and Characterization of *Mycobacterium tuberculosis* Quinolinate Synthase

3.1 Introduction

Mycobacterium tuberculosis is a human pathogen responsible for more than three million deaths per year, making it an important target for biomedical research [1]. Quinolinate synthase (NadA), a key protein in the biosynthetic pathway for the ubiquitous cofactor nicotinamide adenine dinucleotide (NAD), has been isolated from the model organisms *Escherichia coli* [2, 3] and *Arabidopsis thaliana* [4, 5], but not in an organism with the potential impact of *M. tuberculosis*. Early evidence suggested that this organism lacks the salvage pathways that allow it to utilize nicotinic acid as an NAD precursor; thus, it must form its necessary NAD *de novo* through the pathway involving NadA [1].

E. coli NadA was found to contain one $[4\text{Fe-4S}]^{2+}$ cluster per polypeptide, which is purported to be involved in the catalytic mechanism of generating QA from IA and DHAP [2, 3]. The protein contains nine cysteine residues, each of which could potentially serve as a ligand to the cluster, positioning it appropriately for catalysis in the active site. Three of the cysteine residues lie in a $\text{C}^{291}\text{XXC}^{294}\text{XXC}^{297}$ motif similar to that found in other Fe/S cluster proteins. However, the cysteine residues that ligate the NadA cluster are 113, 200, and 297, only one of which (C297) lies in the characteristic motif (unpublished results). These residues are highly conserved among species, including *M. tuberculosis*, which contains 10 cysteine residues, but no CXXCXXC motif.

Thus, it is proposed that WT *M. tuberculosis* NadA will also contain an iron-sulfur cluster necessary for catalysis. Changing any of the conserved cysteine residues, 114, 201, or 300, to alanine will result in protein that is lacking the cluster and unable to perform catalysis. In addition, understanding of this enzyme may provide the foundation for the development of new tuberculosis drugs.

3.2 Materials and Methods

Materials

All DNA modifying enzymes and reagents were purchased from New England Biolabs (Beverly, MA). PfuUltraTM High Fidelity DNA Polymerase and its associated 10× reaction buffer were obtained from Stratagene (La Jolla, CA). Oligonucleotide primers for cloning were obtained from Integrated DNA Technologies (Carlsbad, CA). *Mycobacterium tuberculosis* genomic DNA (strain H37Rv) was obtained from Mycobacterial Research Laboratories at Colorado State University. Coomassie blue dye-binding reagent for protein concentration determination and the bovine serum albumin (BSA) standard (2 mg mL⁻¹) were obtained from Pierce (Rockford, IL). Nickel nitrilotriacetic acid (Ni-NTA) resin was purchased from Qiagen (Valencia, CA), and Talon metal affinity resin was purchased from Clontech (Mountain View, CA). Sephadex G-25 resin and PD-10 pre-poured gel filtration columns were purchased from GE Biosciences (Piscataway, NJ). 2,3-Pyridinedicarboxylic acid (quinolinic acid standard) was obtained from Aldrich (St. Louis, MO). Dihydroxyacetone phosphate (dilithium salt) was obtained from Sigma (St. Louis, MO), and *o*-phenanthroline was obtained from Fisher (Fair Lawn, NJ). All other buffers and chemicals were of the highest grade available. ⁵⁷Fe (97-98%) metal was purchased from Isotopex USA (San

Francisco, CA). It was washed with CHCl_3 and dissolved with heating in an anaerobic solution of 2 N H_2SO_4 (1.5 mol of H_2SO_4 per mole of ^{57}Fe). Prior to use for reconstitution, it was titrated to pH 6.5 with an anaerobic solution of saturated sodium bicarbonate.

General Procedures

High performance liquid chromatography (HPLC) was conducted on a Beckman System Gold unit (Fullerton, CA), which was fitted with a 128 diode array detector and operated with the System Gold *Nouveau* software package. Iron and sulfide analysis was performed as previously described [6, 7]. Sonic disruption of *E. coli* cells was carried out with a 550 sonic dismembrator from Fisher Scientific (Pittsburgh, PA) in combination with a horn containing a ½ in. tip.

Spectroscopic Methods

UV-visible spectra were obtained on a Cary 50 spectrometer (Varian; Walnut Creek, CA) using the associated WinUV software package. Low-temperature X-band EPR spectroscopy was carried out in perpendicular mode on a Bruker (Billerica, MA) ESP 300 spectrometer equipped with an ER 041 MR microwave bridge and an ST4102 X-band resonator (Bruker). The sample temperature was maintained with an ITC503S temperature controller and an ESR900 liquid helium cryostat (Oxford Instruments; Concord, MA).

Mössbauer spectra were recorded on spectrometers from WEB research (Edina, MN) operating in constant acceleration mode in transmission geometry. Spectra were recorded with the temperature maintained at 4.2 K. The sample was kept inside an SVT-400 dewar from Janis (Wilmington, MA), and a magnetic field of 40 mT was applied

parallel to the γ -beam. The isomer shift is relative to the centroid of the spectrum of a metallic foil of α -Fe at room temperature. Data analysis was performed using the program WMOSS from WEB research.

Cloning of Mycobacterium tuberculosis nadA

The *nadA* gene was cloned by PCR into a pET28a expression vector, which is isopropyl- β -D-thiogalactopyranoside (IPTG)-inducible, such that the protein contains an N-terminal hexahistidine tag. The *nadA* gene was amplified from *M. tuberculosis* (strain H37Rv) genomic DNA by PCR using the forward primer containing a *Nde*I restriction site and reverse primer containing an *Eco*RI restriction site. The amplification reaction contained the following in a volume of 50 μ L: 0.8 μ M of each primer (see Table 3-1), 0.25 mM of each deoxynucleoside triphosphate, 300 ng of *Mycobacterium tuberculosis* genomic DNA, 2.5 U of PfuUltraTM High Fidelity DNA Polymerase, and 5 μ L of 10 \times PfuUltraTM reaction buffer. The reaction mixture was overlaid with 30 μ L of mineral oil. After a 9 min denaturation step at 95 $^{\circ}$ C, 35 cycles of the following program were initiated: 1 min at 95 $^{\circ}$ C, 1 min at 60 $^{\circ}$ C, 2 min 30 sec at 72 $^{\circ}$ C. The reaction was finalized at 72 $^{\circ}$ C for 10 min. After amplification by PCR, the resulting fragments were digested with *Nde*I and *Eco*RI, and simultaneously ligated into a pET28a expression vector that had been digested with *Nde*I and *Eco*RI. All other procedures were carried out by standard methods. DNA sequencing was carried out at the Pennsylvania State University Nucleic Acid Facility.

Cloning of E. coli NadB

The *nadB* gene was amplified from *E. coli* (strain W3110) genomic DNA by PCR technology using primers nadBfor and nadBrev (see Table 3-1). Each amplification reaction contained the same concentrations of reagents as described above for cloning the *nadA* gene, except that DMSO was added to a final concentration of 4%. After a 2 min denaturation step at 95 °C, 30 cycles of the following program were initiated: 30 sec at 95 °C, 30 sec at 63 °C, 3 min at 72 °C. Following the cycling program, the reaction was incubated further for 10 min at 72 °C. The PCR product was digested with *NdeI* and *HindIII* and then ligated into similarly digested pET-28a by standard methods. All other procedures were carried out by standard methods. DNA sequencing was carried out at the Pennsylvania State University Nucleic Acid Facility.

Construction of the NadA Variants

The *M. tuberculosis* NadA site-specific variants were constructed using the QuikChange PCR mutagenesis kit (Stratagene); the Mt *nadA* gene cloned into pET28a served as the template, and the forward and reverse primers for each amino acid substitution are listed in Table 3-1.

| Primer | Sequence | Purpose |
|-----------------------|--|---|
| MTnadA.for | 5'-CGC GGC GTC <u>CAT</u> ATG GTG CTG AAT CGC ACG GAC ACG C-3' | Forward primer for <i>Mt nadA</i> ^a |
| MTnadA.rev nadBfor | 5'-CGC GGC GTC <u>GAA</u> TTC TCA TTC GCC ACC GCC GGG ATG CGG G-3' | Reverse primer for <i>Mt nadA</i> ^b |
| nadBrev | 5'-GCG GCG TCC <u>ATA</u> TGA ATA CTC TCC CTG AAC ATT CAT GTG ACG TGT TGA TTA TCG G-3' | Forward Primer for <i>E. coli nadB</i> ^a |
| | 5'-GCG CGA <u>AGC</u> TTT TAT CTG TTT ATG TAA TGA TTG CCG GGG GAA AGG ATC GAC GG-3' | Reverse primer for <i>E. coli nadA</i> ^c |
| MTnadA C114A for. | 5'-GGA TCA GCG GGC CGG CGC TTC GCT GGC CGA TTC G-3' | Forward primer for C114A |
| MTnadA C114A rev. | 5'-CGA ATC GGC CAG CGA AGC GCC GGC CCG CTG ATC C-3' | Reverse primer for C114A |
| MtNadA C201A For | 5'-GCA TGT GTG GGC CGG CGA AGC CCA CGT ACA CGC CGG GAT CAA CG-3' | Forward primer for C201A |
| MtNadA C201A Rev | 5'-CGT TGA TCC CGG CGT GTA CGT GGG CTT CGC CGG CCC ACA CAT GC-3' | Reverse primer for C201A |
| MtNadA C300A For | 5'-GCG GTC AAC GAC CGC GCC TCA GCC AAG TAC ATG AAG ATG ATC ACC-3' | Forward primer for C300A |
| MtNadA C300A Rev | 5'-GGT GAT CAT CTT CAT GTA CTT GGC TGA GGC GCG GTC GTT GAC CGC-3' | Reverse primer for C300A |
| C87A MtNadA.for.AEG | 5'-GGA CAC CAT CGT GTT CGC CGG AGT GCA CTT CAT GG-3' | Forward primer for C87A |
| C87A MtNadA.rev.AEG | 5'-CCA TGA AGT GCA CTC CGG CGA ACA CGA TGG TGT CC-3' | Reverse primer for C87A |
| C230AMtNadA.for.AEG | 5'-CGA ACT GTT CGT GCA TCC GGA GGC TGG TTG CGC AAC CTC GGC GC-3' | Forward primer for C230A |
| C230AMtNadA.rev.AEG | 5'-GCG CCG AGG TTG CGC AAC CAG CCT CCG GAT GCA CGA ACA GTT CG -3' | Reverse primer for C230A |
| Cter3MtNadA.rev | 5'-CGC GGC GTC <u>CTC</u> GAG TCT TTC GCC ACC GCC GGG ATG GCC G-3' | Reverse primer for cloning <i>nadA</i> ^d |

^a Underlined bases represent *NdeI* restriction site.

^b Underlined bases represent *EcoRI* restriction site.

^c Underlined bases represent *HindIII* restriction site.

^d Underlined bases represent *XhoI* restriction site.

Bolded bases represent amino acid changes.

Table 3-1: Primers used in cloning and mutagenesis of *nadA* genes from *M. tuberculosis*

Expression of WT M. tuberculosis NadA and Variants

The *nadA* gene was cloned by PCR into a pET28a expression vector, which is isopropyl- β -D-thiogalactopyranoside (IPTG)-inducible, such that the protein contains an N-terminal hexahistidine tag. The resulting plasmid was cotransformed into *E. coli* BL21(DE3) along with the plasmid pDB1282, which contains the *Azotobacter vinelandii* *isc* operon cloned behind an arabinose-inducible promoter [8]. This operon includes the important Fe/S cluster assembly genes, *iscS*, *iscU*, *iscA*, *hscA*, *hscB*, and *fdx* [9, 10].

A single colony was used to inoculate 100 mL of Luria–Bertani (LB) media containing 50 μ g/mL kanamycin and 100 μ g/mL ampicillin and was cultured for approximately 7 h at 37 °C with shaking. A 60 mL portion of the culture was then evenly distributed among four 6 L Erlenmeyer flasks to inoculate 16 L of LB media containing 50 μ g/mL kanamycin and 100 μ g/mL ampicillin, and was cultured further at 37 °C with shaking (180 rpm). At an optical density (600 nm; OD₆₀₀) of 0.3, solid arabinose was added to each flask at a final concentration of 0.05 % (w/v). At an OD₆₀₀ of 0.6, solid IPTG and ferric chloride were added to each flask at final concentrations of 200 and 50 μ M, respectively. The cultures were then incubated further at 37 °C with shaking for 4 h. Cells were harvested at 10,000 $\times g$ for 10 min at 4 °C, and the resulting cell paste was frozen in liquid N₂ and stored at -80 °C until ready for use. Typical yields were 60-70 g of cell paste per 16 L growth.

Purification of WT and Variant M. tuberculosis NadA Proteins

All steps of the purification were carried out inside of an anaerobic chamber from Coy Laboratory Products, Inc. (Grass Lake, MI) under an atmosphere of N₂ and H₂

(95%/5%), with an O₂ concentration maintained below 1 ppm by the use of palladium catalysts. Steps using centrifugation were performed outside of the anaerobic chamber in centrifuge tubes that were tightly sealed before removal from the chamber. All buffers were prepared using distilled and deionized water that was boiled for at least 1 h and then allowed to cool uncapped with stirring in the anaerobic chamber for 48 h. All plastic ware was autoclaved and brought into the chamber hot and allowed to equilibrate overnight before use.

Protein purification was carried out by immobilized metal affinity chromatography using a nickel-nitrilotriacetic acid (Ni-NTA) matrix. In a typical purification, 25 g of frozen cells were resuspended in 80 mL of buffer A (50 mM HEPES, pH 7.5, 0.3 M KCl, 20 mM imidazole, and 10 mM 2-mercaptoethanol). Solid egg white lysozyme was added to a final concentration of 1 mg mL⁻¹ and the mixture was stirred at room temperature for 30 min. After the solution was cooled in an ice-water bath to <8 °C, it was subjected to 4 cycles of a 1 min burst of sonic disruption (setting 7), with intermittent pausing to allow the temperature to re-equilibrate to <8 °C. Cellular debris was removed by centrifugation at 50,000 × g for 1 h and the supernatant was loaded onto a Ni-NTA column (2.5 x 7 cm) equilibrated in buffer A. The column was washed with 100 mL of buffer B (50 mM HEPES, pH 7.5, 0.3 M KCl, 40 mM imidazole, 10 mM 2-mercaptoethanol, and 20% glycerol) before eluting with buffer B containing 250 mM imidazole. Fractions that were brown in color were pooled and concentrated in an Amicon stirred cell (Millipore, Billerica, MA) fitted with a YM-10 membrane (10,000 Da MW cutoff). The protein was exchanged into buffer C (50 mM HEPES, pH 7.5, 0.1 M KCl, 10 mM DTT and 20% glycerol) by anaerobic gel filtration (Sephadex G-25),

concentrated, and stored in aliquots in a liquid N₂ dewar until ready for use, or immediately reconstituted (see below) with iron and sulfide. All buffers were chilled on ice prior to use and ice packs were used to jacket the Amicon stirred cell during protein concentration.

Reconstitution of NadA

Reconstitution of NadA with iron and sulfide was carried out on ice in a Coy anaerobic chamber using anaerobic buffers and solutions. A typical reconstitution contained, in a final volume of 20 mL, 100 μ M NadA that was initially treated with 5 mM DTT for 20 min. An 8-fold molar excess of FeCl₃ was added and the solution was allowed to sit on ice for 20 mins. Finally, an 8-fold molar excess of Na₂S was added over a period of 3 to 4 h, which was followed by incubation on ice for at least 5 h to a maximum of 13 h (overnight). The solution was then concentrated in an Amicon stirred cell, placed in airtight centrifuge tubes, removed from the anaerobic chamber, and centrifuged at 14,000 $\times g$ for 2 min to remove precipitate. The reconstituted (RCN) samples were brought back into the anaerobic chamber, and the supernatants were removed and exchanged into buffer C by gel filtration (Sephadex G-25 or Amersham PD-10), reconcentrated, and stored in aliquots in a liquid N₂ dewar.

Expression and Purification of E. coli NadB

The *nadB* gene was cloned by PCR into a pET-28a expression vector such that the protein is produced with an N-terminal hexahistidine tag, and transformed into *E. coli* BL21(DE3). A single colony was used to inoculate 100 mL of Luria–Bertani (LB) media containing 50 μ g/mL kanamycin and was cultured for 7 h at 37 °C with shaking. A 60 mL portion of the culture was evenly distributed among four 6 L Erlenmeyer flasks to

inoculate 16 L of LB media containing 50 $\mu\text{g/mL}$ kanamycin and was cultured further at 37 °C. At an OD_{600} of 0.6, the cultures were cooled in an ice-water bath, and solid IPTG and FAD were added to each flask to final concentrations of 200 and 10 μM , respectively. The cultures were then incubated at 18 °C with shaking for 16 h. Cells were harvested at $10,000 \times g$ for 10 min at 4 °C, affording typical yields of 50-60 g of cell paste, which was frozen in liquid N_2 and stored at -80 °C until ready for use.

In a typical purification, 25 g of frozen cells were resuspended in 80 mL of buffer D (50 mM HEPES, pH 7.5, 0.2 M NaCl, 10 mM imidazole, 10 mM succinate, pH 8, and 20 μM FAD). Solid egg white lysozyme and phenylmethanesulfonyl fluoride (PMSF) were added to final concentrations of 1 mg mL^{-1} and 1 mM, respectively, and the mixture was stirred at room temperature for 30 min. After the solution was cooled in an ice-water bath to <8 °C, it was subjected to four 1 min bursts of sonic disruption (setting 7), with intermittent pausing between bursts to allow the temperature to return to <8 °C. Cellular debris was removed by centrifugation at $50,000 \times g$ for 1 h and the supernatant was loaded onto a Ni-NTA column (2.5 x 7 cm) equilibrated in buffer D. The column was washed with 175 ml of buffer E (50 mM HEPES, pH 7.5, 0.2 M NaCl, 20 mM imidazole, 10 mM succinate, pH 8, 20 μM FAD, and 10% glycerol) and subsequently eluted with buffer E containing 250 mM imidazole. Protein-containing fractions were pooled and concentrated in an Amicon stirred cell (Millipore, Billerica, MA) fitted with a YM-10 membrane (10,000 Da MW cutoff). The protein was exchanged into anaerobic buffer F (50 mM HEPES, pH 7.5, and 10% glycerol) by anaerobic gel filtration (Sephadex G-25),

reconcentrated, and stored in aliquots in a liquid N₂ dewar until ready for use.

Determination of Protein Concentration

Protein concentrations were determined by the Bradford dye staining procedure with BSA as the standard (11). For WT *M. tuberculosis* NadA, parallel samples were subjected to quantitative amino acid analysis at the University of Iowa Molecular Analysis Facility to confirm that the Bradford assay was accurate without a correction factor.

Assay for Quinolinic Acid

The activity of WT and variant NadA proteins was determined by monitoring the formation of QA over a twenty-minute time period at 37 °C under anaerobic conditions. The substrate IA was generated either enzymatically from L-aspartate by NadB using fumarate as the electron acceptor, or chemically by reacting OAA with ammonium sulfate [12]. The assay using the enzymatically generated iminoaspartate contained, in a final volume of 1300 µL, 200 mM HEPES, pH 7.5, 25 mM L-aspartate/fumarate solution, pH 7, 25 µM FAD, 1 mM DHAP, 0.1 M KCl, 0.3 mM L-tryptophan (internal standard), and either 5 µM NadA (RCN enzyme) and 5 µM NadB or 15 µM NadA (AI enzyme) and 15 µM NadB. In the assay using chemically generated IA, the aspartate/fumarate solution, FAD, and NadB were replaced with 10 mM OAA and 100 mM ammonium sulfate. The reactions were initiated by addition of either NadB or OAA after incubation of the other components in the assay mixture at 37 °C for 5 min. At designated times, 200 µL aliquots of the assay mixture were removed and added to 40 µL of 2 M trichloroacetic acid to quench the reaction. The precipitated protein was pelleted by

centrifugation and the supernatant was analyzed by HPLC with UV detection (268 nm) using a Zorbax SB-C18 column (4.6 x 250 mm), which was obtained from Agilent. The column was equilibrated in 100% Solvent A (1% TFA) at a flow rate of 1 mL min⁻¹. These initial conditions were maintained for 10 min after injection, after which a gradient of 0-45% Solvent B (acetonitrile) was applied over 10 min. At 20 min, a gradient of 45-90% Solvent B was applied over 3 min. Finally, at 25 min, a gradient of 90-0% Solvent B was applied over 3 min to re-establish the initial conditions until the end of the run at 32 min. Using this method, QA eluted at 8.3 min and the tryptophan internal standard eluted at 20.3 min. The concentration of QA was determined from a calibration curve of known concentrations of QA, using the internal standard to correct for volume changes between sample injections.

Preparation of Mössbauer and EPR Samples

In order to analyze samples by Mössbauer spectroscopy, cells were cultured in M9 minimal media. In addition, ⁵⁷FeSO₄ was substituted for FeCl₃. All other growth and purification procedures were as described above. Mössbauer samples (400 µL total volume) were prepared in small plastic cups before freezing in liquid N₂. EPR samples (250 µL total volume) of reduced *M. tuberculosis* NadA were treated with 2 mM sodium dithionite at room temperature for approximately 5 min prior before loading into EPR tubes (2 mm i.d.) and freezing in liquid nitrogen. Samples analyzed contained 250-450 µM NadA and were all prepared inside of the anaerobic chamber.

3.3 Results

Expression of M. tuberculosis NadA

The *M. tuberculosis nadA* gene was cloned into an IPTG-inducible pET28a vector such that the protein would contain an N-terminal hexahistidine tag, and the resulting construct was cotransformed into *E. coli* BL21 (DE3) cells along with the arabinose-inducible plasmid pDB1282 containing the *A. vinelandii isc* operon. Although expression of the *isc* genes is not observed, the *nadA* gene is clearly expressed after a 4 h induction at 37 °C, as shown by production of a ~40 kDa protein by SDS-PAGE (Figure 3-1, Lane 4). The resulting cell paste was brown in color, and obtained in a yield of 4-5 g per liter of media. Unlike the *E. coli* NadA protein, very little expression was seen if the protein was induced for 16 h at 18° C.

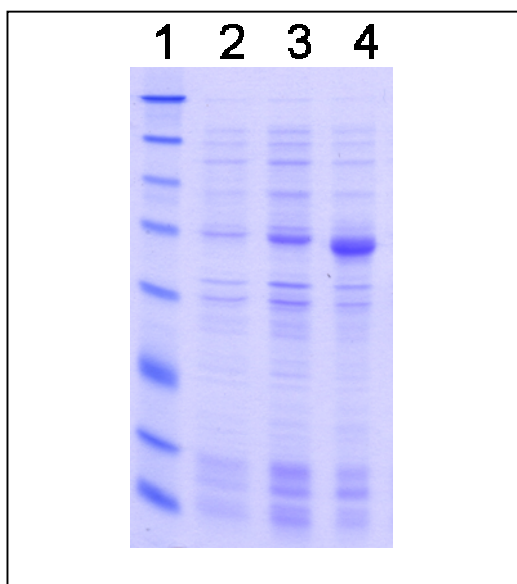


Figure 3-1: SDS-PAGE of *M. tuberculosis* NadA expression

Lane 1: molecular weight standards (from top); 175, 83, 62, 47.5, 32.5, 25, 16.5 6.5 kDa;
Lane 2: at OD₆₀₀ 0.3; Lane 3: at OD₆₀₀ 0.6; Lane 4: after 4 hour induction

Purification and Characterization of WT M. tuberculosis NadA

M. tuberculosis NadA was successfully isolated under anaerobic conditions using a procedure similar to that used for isolating *E. coli* NadA [2]. The protein was highly soluble, with little protein apparent in the pellet after centrifugation (Figure 3-2, lane 3). The final protein was obtained in a yield of about 1-1.5 mg of protein per gram of cell paste. It was dark brown in color and essentially homogeneous as determined by SDS-PAGE (Figure 4-3, lane 6). The UV-visible spectral envelope was consistent with the presence of a [4Fe-4S] cluster, as it contained a shoulder at ~320 nm, a peak at ~400 nm, and broad tailing that extended beyond 700 nm, in addition to the typical protein peak at 280 nm. (Figure 3-3, solid line). Iron and sulfide quantification of this protein indicated the presence of 4.7 ± 0.2 equivalents of iron per protein, and 2.6 ± 0.1 of sulfide per polypeptide. These numbers are consistent with the presence of one [4Fe-4S] cluster per polypeptide, as previously found for the *E. coli* protein [2]. Chemical reconstitution of the AI protein resulted in an increase in the UV-visible absorbance at 400 nm (Figure 3-3, dashed line), as well as the iron and sulfide content, which was present at 6.4 ± 0.0 equiv and 2.7 ± 0.1 equiv per polypeptide, respectively.

Using 15 μ M NadA and 15 μ M NadB, AI NadA catalyzed the formation of QA with a $V_{\max}/[E_T]$ of 0.24 min^{-1} , while reconstituted enzyme exhibited rates that were generally two-fold higher. When using chemically generated IA and AI enzyme, rates were typically 1.5-fold higher than those achieved with the enzymatically generated aspartate.

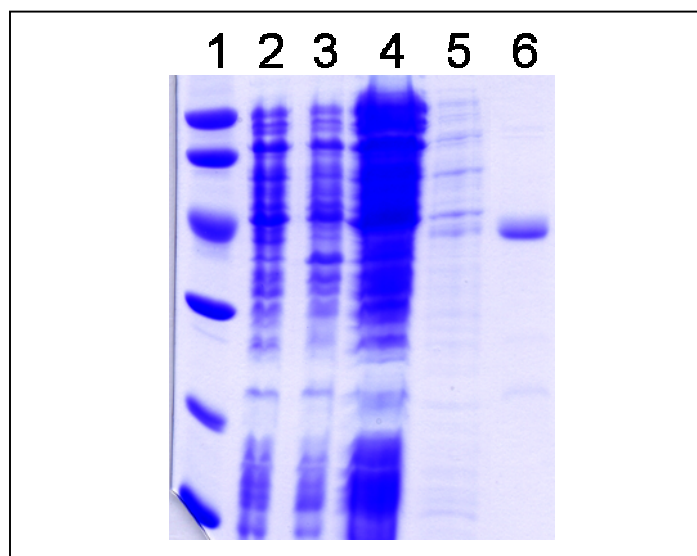


Figure 3-2: SDS-PAGE of WT *M. tuberculosis* NadA purification

Lane 1: molecular weight standards (from top); 97.0, 66.0, 45.0, 30.0, 20.1, 14.4 kDa;

Lane 2: lysate supernatant; Lane 3: lysate pellet; Lane 4: Ni-NTA load eluate; Lane 5:

Ni-NTA wash eluate; Lane 6: purified protein

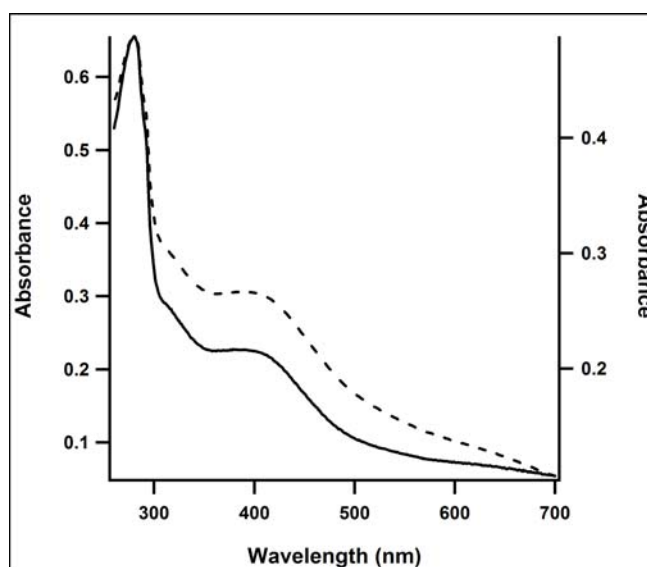


Figure 3-3: UV-visible spectra of WT *M. tuberculosis* NadA, AI (solid line, left axis), and RCN (dashed line, right axis).

Mössbauer and EPR Spectroscopy of M. tuberculosis NadA

To confirm the presence of the cluster, *M. tuberculosis* NadA was expressed in the presence of the isotope ^{57}Fe , allowing for further study by Mössbauer spectroscopy. The 4.2 K Mössbauer spectrum, recorded in a parallel magnetic field of 40 mT was typical for a $[\text{4Fe-4S}]^{2+}$ cluster (Figure 3-4, hashed marks), and could be fitted to a single quadrupole doublet with a quadrupole splitting parameter (ΔE_Q) of 1.13 mm/s and isomer shift (δ) of 0.46 mm/s (solid line, Figure 3-4). EPR spectroscopy of the protein reduced with 2 mM dithionite and recorded at 5 mW power and 13K exhibited a spectrum similar to that seen for reduced, as-isolated wild-type *E. coli* NadA, with g values of 2.06, and 1.92 (Figure 3-5).

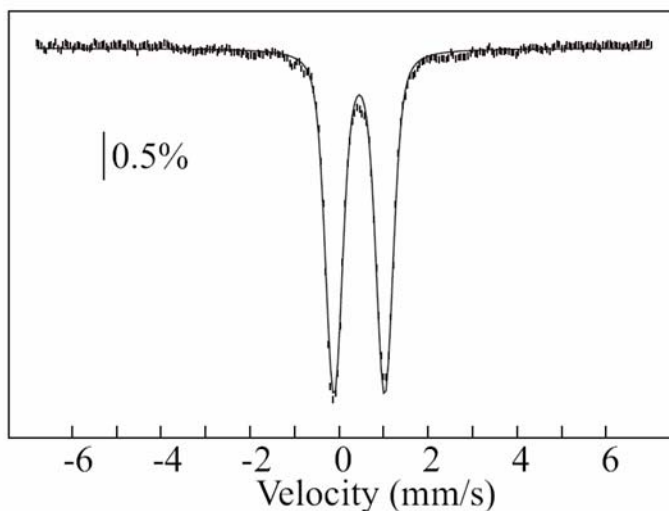


Figure 3-4: Mössbauer spectrum of as-isolated ^{57}Fe *M. tuberculosis* NadA (hashed marks indicate experimental data, solid line represents fitting)

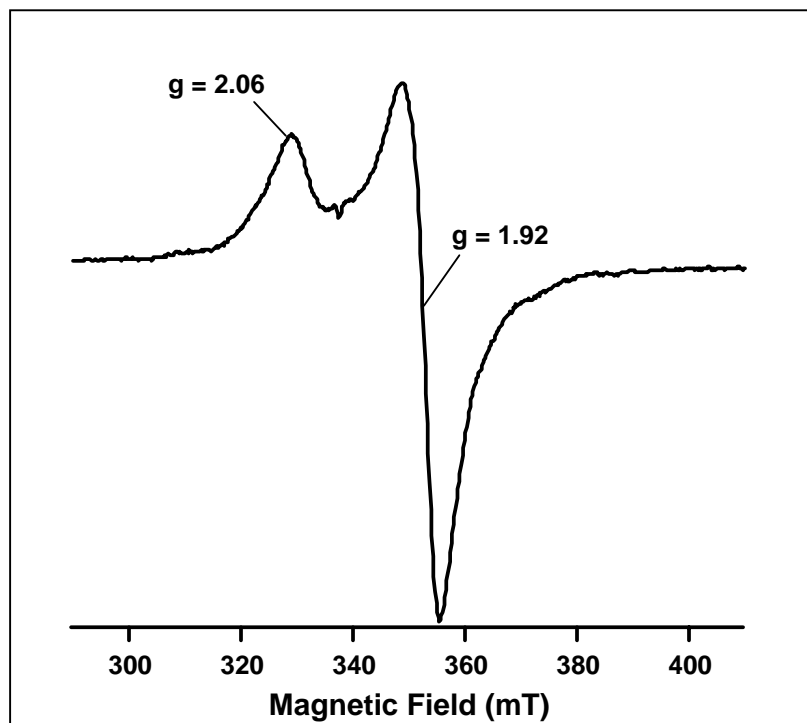


Figure 3-5: EPR spectrum of reduced as-isolated *M. tuberculosis* NadA

Variants of M. tuberculosis NadA

Site-directed mutagenesis was used to generate variant proteins of *M. tuberculosis* NadA in which the three highly conserved cysteines, 300, 201, and 114, were individually changed to alanine residues. Mutations were confirmed by DNA sequencing prior to cotransformation with pDB1282 into BL21(DE3) cells. Subsequent expression studies showed a level of protein expression similar to that of wild-type *M. tuberculosis* NadA. However, the proteins were unable to be purified using the procedure used to isolate the *M. tuberculosis* wild-type, *E. coli* wild-type, and *E. coli* variant proteins. The lysate supernatant was more yellow than brown in color, which is attributed to the *iscS* protein encoded by the pDB1282 plasmid, which has a molecular mass similar to NadA. The variant protein is isolated in the pellet after centrifugation, as shown by the large band at ~45 kDa. Lane 6 of Figure 3-6 contains the sample that was eluted from the Ni-

NTA column with high imidazole buffer. Although several bands are seen, none are at the ~40 kDa molecular mass expected for NadA. While the SDS-PAGE gel in Figure 3-6 represents the C114A variant, identical results, including the same bands at approximately 66, 28 and 24 kDa in the final sample, were observed with the C300A and C201A variants. Similar results were also seen with variants C230A and C87A, in which cysteine residues hypothesized to be uninvolved in cluster ligation were changed. Use of Talon metal affinity resin, which is more specific for the hexahistidine tag, did not improve the purification, supporting the evidence that NadA is produced in the pellet.

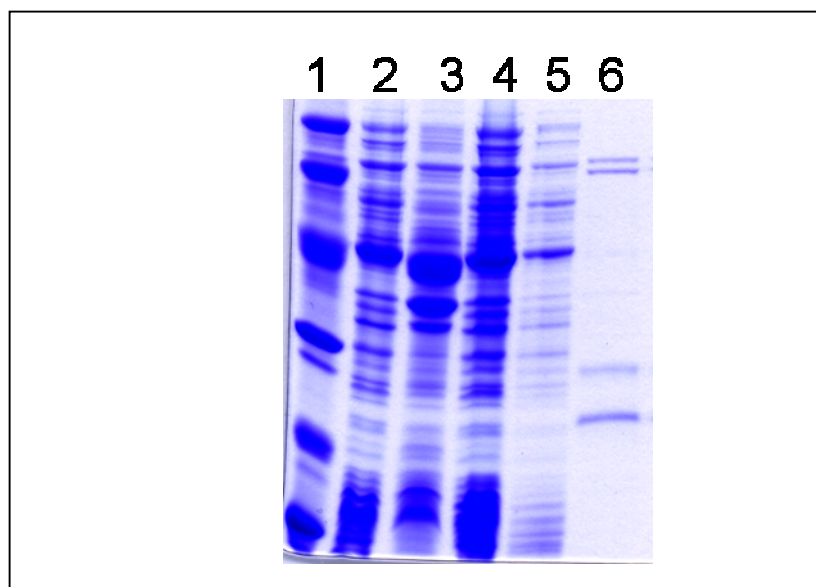


Figure 3-6: SDS-PAGE of C114A *M. tuberculosis* NadA purification

Lane 1: molecular weight standards (from top); 97.0, 66.0, 45.0, 30.0, 20.1, 14.4 kDa;
Lane 2: lysate supernatant; Lane 3: lysate pellet; Lane 4: Ni-NTA load eluate; Lane 5:
Ni-NTA wash eluate; Lane 6: purified protein

3.4 Discussion

Mycobacterium tuberculosis NadA was found to have characteristics very similar to the *E. coli* NadA protein previously studied. The *M. tuberculosis* protein does in fact contain a $[4\text{Fe-4S}]^{2+}$ cluster, although it lacks the CXXCXXC motif found in the *E. coli* protein sequence. The cysteines in this motif often ligate the cluster in Fe/S cluster proteins. However, it was found that the cysteine residues that actually ligate the cluster in *E. coli* NadA are not those in the motif, but the three highly conserved residues, cysteines 113, 200, and 297, only one of which lies in the motif (unpublished results). Although *M. tuberculosis* NadA does not contain the motif, it does contain the three conserved cluster-ligating cysteines; thus, it is not surprising that the protein contains an Fe/S cluster. It is hypothesized that the cluster will also be conserved across species, since three cysteines are universally conserved in all annotated quinolinate synthases.

The *M. tuberculosis* NadA sequence contains a total of 10 cysteine residues, one more than found in the *E. coli* NadA sequence. In order to confirm that the three cluster-ligating cysteines were those conserved across species—cysteines 114, 201, and 300—a site-directed mutagenesis approach was used to generate variant proteins lacking one of these cysteines. The variant proteins were expected to have reduced amounts of iron and sulfide per protein, different spectral features, and no quinolinate synthase activity. A similar study had been used to successfully identify the essential cysteines in the *E. coli* protein. Unexpectedly, changing any one of the three cysteines in *M. tuberculosis* NadA resulted in protein which was significantly less stable, and resulted in the formation of inclusion bodies. Variants C230A and C87A, in which the cysteines changed are purported to be uninvolved in cluster ligation, also gave similar results. In all cases,

SDS-PAGE analysis of the eluate collected from a high imidazole wash of the column showed the same series of bands, at molecular masses of approximately 66, 28 and 24 kDa, suggesting that these proteins may be associated with use of the pDB1282 plasmid. The same result was seen when Talon metal affinity resin was substituted for Ni-NTA resin.

In a further attempt to isolate the variant proteins, the N-terminal hexahistidine tag was replaced with a C-terminal hexahistidine tag. The C-terminally tagged protein was also insoluble, and found in inclusion bodies. Treatment of the insoluble protein with 6M urea, followed by on-column refolding of the protein by decreasing the urea concentration, resulted in small quantities of variant NadA protein insufficient for further study. Although *M. tuberculosis* NadA is much more sensitive to individual cysteine residue changes than *E. coli* protein, it was confirmed that the WT protein contains one $[4\text{Fe-4S}]^{2+}$ cluster per protein, demonstrating that the CXXCXXC motif is not required for the cluster to be present.

3.5 References

1. Sharma, V., Grubmeyer, C., Sacchettini, J. C. (1998) Crystal structure of quinolinic acid phosphoribosyltransferase from *Mycobacterium tuberculosis*: A potential TB drug target. *Structure* 6, 1587-1599.
2. Cicchillo, R. M., Tu, L., Stromberg, J. A., Hoffart, L. M., Krebs, C., and Booker, S. (2005) *Escherichia coli* quinolinate synthetase does indeed harbor a $[4\text{Fe-4S}]$ cluster. *J. Am. Chem. Soc.* 127, 7310-7311.

3. Ollagnier-de Choudens, S., Loiseau, L., Sanakis, Y., Barras, F., and Fontecave, M. (2005) Quinolinate synthetase, an iron-sulfur enzyme in NAD biosynthesis. *FEBS Lett.* 579, 3737-3743.
4. Murthy, U. M., N., Ollagnier-de-Choudens, S., Sanakis, Y., Abdel-Ghany, S. E., Rousset, C., Ye, H., Fontecave, M., Pilon-Smits, E. A. H., and Pilon, M. (2007) Characterization of *Arabidopsis thaliana* SufE2 and SufE3: Functions in chloroplast iron-sulfur cluster assembly and NAD synthesis. *J. Biol. Chem.* 282, 18254-18264.
5. Katoh, A., Uenohara, K., Akita, M., and Hashimoto, T. (2006) Early steps in the biosynthesis of NAD in arabidopsis start with aspartate and occur in the plastid. *Plant Physiol.* 141, 851-857.
6. Beinert, H. (1978) Micro methods for the quantitative determination of iron and copper in biological material. *Methods Enzymol.* 54, 435-445.
7. Beinert, H. (1983) Semi-micro methods for analysis of labile sulfide and of labile sulfide plus sulfane sulfur in unusually stable iron-sulfur proteins. *Anal. Biochem.* 131, 373-378.
8. Kriek, M. M., Peters, L. L., Takahashi, Y. Y., and Roach, P. L. (2003) Effect of iron-sulfur cluster assembly proteins on the expression of *Escherichia coli* lipoic acid synthase. *Prot. Express. Purif.* 28, 241-245.
9. Frazzon, J., Fick, J. R., and Dean, D. R. (2002) Biosynthesis of iron-sulphur clusters is a complex and highly conserved process. *Biochem. Soc. Trans.* 30, 680-685.

10. Frazzon, J., and Dean, D. R. (2003) Formation of iron-sulfur clusters in bacteria: an emerging field in bioinorganic chemistry. *Curr. Opin. Chem. Biol.* 7, 166-173.
11. Nasu, S., and Gholson, R. K. (1981) Replacement of the B protein requirement of the *E. coli* quinolinate synthetase system by chemically-generated iminoaspartate. *Biochem. Biophys. Res. Commun.* 101, 533-539.
12. Bradford, M. M. (1976) A rapid and sensitive method for the quantitation of microgram quantities of protein utilizing the principle of protein-dye binding. *Anal. Biochem.* 72, 248 - 254.

Chapter 4:

Cloning, Purification, and Characterization of *Pyrococcus horikoshii* Quinolinate Synthase

4.1 Introduction

Quinolinate synthase (NadA) is responsible for the formation of QA, a key intermediate in the biosynthetic pathway of the essential cofactor, nicotinamide adenine dinucleotide. Most prokaryotes, unlike most eukaryotes, generate QA from L-aspartate via a pathway that is not strictly dependent on the use of molecular oxygen as a cosubstrate. The flavoprotein L-aspartate oxidase, or NadB, catalyzes the two-electron oxidation of L-aspartate to the unstable intermediate, IA. *In vitro*, IA can also be generated chemically by combining ammonia and OAA [1]. NadA then catalyzes a condensation reaction between IA and DHAP, generating QA, 2 molecules of water, and P_i . Quinolinate synthase belongs to the hydro-lyase family of enzymes, some of which require an Fe/S cluster for catalysis [2].

Recent studies of NadA from *E. coli* determined that the protein contained one $[4Fe-4S]^{2+}$ cluster per polypeptide [3, 4], in contrast to initial studies on the recombinant enzyme, in which turnover was observed presumably in the absence of cluster (Ceciliani, 2000). It was hypothesized that the cluster would serve a role similar to that in the hydro-lyase enzyme aconitase. The aconitase Fe/S cluster is ligated by three cysteine residues that coordinate three iron atoms; the fourth iron site (Fe_a), which is coordinated by a hydroxo or water ligand, is open to coordinate substrate and facilitate catalysis. The substrate binds to Fe_a in a bidentate fashion with a change in geometry from tetrahedral to octahedral. In the same vein, NadA contains only three cysteines that are strictly

conserved and required for activity, suggesting that they are the residues that serve as ligands to the [4Fe-4S] cluster (unpublished results).

Recently, Sakuraba et al. determined and published the first crystal structure of a quinolinate synthase, and in fact the only structure of a cluster-containing hydro-lyase other than aconitase [6]. The protein was obtained from the hyperthermophilic archaeon *Pyrococcus horikoshii*, and shows three analogous domains centered around a pseudo three-fold axis. This structure could have provided valuable insight about the quinolinate synthase mechanism and the role of the cluster in catalysis; however, it did not contain an Fe/S cluster, and this important cofactor was not mentioned in the paper. Furthermore, the structure also contained three regions that were not resolved in electron density maps. Interestingly, each of these disordered loop regions lies near one of the three highly conserved cysteine residues found to ligate the cluster in *E. coli* NadA, as shown in the sequence alignment of *E. coli* and *P. horikoshii* proteins (Figure 4-1).

| | | | | |
|----|--|------------------------------|---------------------------------------|---------------------------|
| Ec | MGETAKILSPEKTILMPTLQAECSLDLGC | CPVEEFNAFC | DAHPDRTVVVYANTSAAVKARA | |
| Ph | MAETAKILNPKVVLIP | PSREATC | AMANMLKVEHILEAKRKYPNAPVVLVYNSTAEAKAYA | |
| Ec | DWVVTSSIAVELIDHLD | SLGEKIIWAPDKHLGRYVQKQTGGDILC | W--QGAC | IVHDEFKT |
| Ph | DVTVTSANAVEVVKLDS-- | DVVIFGPDKNLAHYVAKMTGKKII | PVPSKGHC | YVHQKFTL |
| Ec | QALTRLQEEYPDAAILVHPESPQAIVDMADAVGSTSQLIAAAKTLPHQRLIVATDRGIFY | | | |
| Ph | DDVERAKKLHPNAKLMIHPEC | IPEVQEKADIIASTGGMI-- | KRAC | EWDEWVVFTEREMVY |
| Ec | KMQQAVPDKELLEAPTAGEGATCR | SCAHC | CPWMAMNGLQAI | AEALEQEGSNHEVHVDERLR |
| Ph | RLRKLYPQKKFYPA----- | REDAFC | IGMKA | ITLKNYESLKDM--KYKVEVPEEIA |

Figure 4-1: Sequence alignment of *E. coli* and *P. horikoshii* quinolinate synthases (cysteines in yellow, blue residues indicate unresolved residues)

The work described here establishes an expression and purification scheme for the *P. horikoshii* NadA protein with consideration for the Fe/S cluster and its oxygen sensitivity. The purified protein was characterized, and results confirmed that *P. horikoshii* NadA does in fact contain one $[4\text{Fe-4S}]^{2+}$ cluster per polypeptide, and furthermore, that this cluster is absolutely essential for the catalytic formation of QA. Purification of the protein with intact cluster should also stabilize the previously observed disordered regions of the protein, allowing a complete *P. horikoshii* NadA structure to be solved.

4.2 Materials and Methods

Materials

All DNA modifying enzymes and reagents, and Deep Vent DNA Polymerase and its associated 10x ThermoPol reaction buffer were purchased from New England Biolabs (Beverly, MA). PfuUltra™ High Fidelity DNA Polymerase and its associated 10×

reaction buffer were obtained from Stratagene (La Jolla, CA). Oligonucleotide primers for cloning were obtained from Integrated DNA Technologies (Carlsbad, CA). *Pyrococcus horikoshii* genomic DNA (JCM 9974) was obtained from ATCC (Manassas, VA). Coomassie blue dye-binding reagent for protein concentration determination and the bovine serum albumin (BSA) standard (2 mg mL^{-1}) were obtained from Pierce (Rockford, IL). Nickel nitrilotriacetic acid (Ni-NTA) resin was purchased from Qiagen (Valencia, CA). Sephadex G-25 resin pre-poured gel filtration columns were purchased from GE Biosciences (Piscataway, NJ). 2,3-Pyridinedicarboxylic acid (quinolinic acid standard) was obtained from Aldrich (St. Louis, MO). Dihydroxyacetone phosphate (dilithium salt) was obtained from Sigma (St. Louis, MO), and *o*-phenanthroline was obtained from Fisher (Fair Lawn, NJ). All other buffers and chemicals were of the highest grade available. ^{57}Fe (97-98%) metal was purchased from Isotrex USA (San Francisco, CA). It was washed with CHCl_3 and dissolved with heating in an anaerobic solution of 2 N H_2SO_4 (1.5 mol of H_2SO_4 per mole of ^{57}Fe). Prior to use for reconstitution, it was titrated to pH 6.5 with an anaerobic solution of saturated sodium bicarbonate.

General Procedures

High performance liquid chromatography (HPLC) was conducted on a Beckman System Gold unit (Fullerton, CA), which was fitted with a 128 diode array detector and operated with the System Gold *Nouveau* software package. Iron and sulfide analysis was performed as previously described [7-9]. Sonic disruption of *E. coli* cells was carried out with a 550 sonic dismembrator from Fisher Scientific (Pittsburgh, PA) in combination with a horn containing a $\frac{1}{2}$ in. tip.

Spectroscopic Methods

UV-visible spectra were obtained on a Cary 50 spectrometer (Varian; Walnut Creek, CA) using the associated WinUV software package. Low-temperature X-band EPR spectroscopy was carried out in perpendicular mode on a Bruker (Billerica, MA) ESP 300 spectrometer equipped with an ER 041 MR microwave bridge and an ST4102 X-band resonator (Bruker). The sample temperature was maintained with an ITC503S temperature controller and an ESR900 liquid helium cryostat (Oxford Instruments; Concord, MA).

Mössbauer spectra were recorded on spectrometers from WEB research (Edina, MN) operating in constant acceleration mode in transmission geometry. Spectra were recorded with the temperature maintained at 4.2 K. The sample was kept inside an SVT-400 dewar from Janis (Wilmington, MA), and a magnetic field of 40 mT was applied parallel to the γ -beam. The isomer shift is relative to the centroid of the spectrum of a metallic foil of α -Fe at room temperature. Data analysis was performed using the program WMOSS from WEB research.

*Cloning of the *Pyrococcus horikoshii* nadA gene*

The *nadA* gene was amplified from *P. horikoshii* (JCM 9974) genomic DNA by PCR using the forward primer 5'-CGC-GGC-GTC-CAT-ATG-GAT-TTA-GTT-GAA-GAA-ATT-TTG-AGG-CTT-AAA-GAG-G-3' (*Nde*I restriction site underlined) and reverse primer 5'-CGC-GGC-GTC-GAA-TTC-TCA-TTT-GCT-CAT-CTC-CAG-CAT-TCT-TTC-TAT-GGC-3' (*Eco*RI restriction site underlined). Each amplification reaction contained the following in a volume of 50 μ L: 0.48 μ M of each primer, 0.25 mM of each deoxynucleoside triphosphate, 200 ng of *Pyrococcus horikoshii* genomic DNA, 2 U of

Deep Vent DNA Polymerase, and 5 μ L of 10 \times ThermoPol reaction buffer. The reaction mixture was overlaid with 40 μ L of mineral oil. After a 9 min denaturation step at 95 $^{\circ}$ C, 35 cycles of the following program were initiated: 1 min at 95 $^{\circ}$ C, 1 min at 55 $^{\circ}$ C, 2.5 min at 72 $^{\circ}$ C. The reaction was finalized at 72 $^{\circ}$ C for 10 min. The PCR product was digested with *Nde*I and *Eco*RI and then ligated into a pET28a expression vector digested with the same enzymes.

Expression of P. horikoshii NadA

The *nadA* gene was cloned by PCR into a pET28a expression vector, which is isopropyl- β -D-thiogalactopyranoside (IPTG)-inducible, such that the protein contains an N-terminal hexahistidine tag. The plasmid was cotransformed into *E. coli* BL21 (DE3) Rosetta2 cells along with the plasmid pDB1282, which contains the *Azotobacter vinelandii* *isc* operon cloned behind an arabinose-inducible promoter [10]. This operon includes the important Fe/S cluster assembly genes, *iscS*, *iscU*, *iscA*, *hscA*, *hscB*, and *fdx* [11, 12].

A single colony was used to inoculate 100 mL of Luria–Bertani (LB) media containing 50 μ g/mL kanamycin, 100 μ g/mL ampicillin, and 34 μ g/mL chloramphenicol, and was cultured for approximately 7 h at 37 $^{\circ}$ C with shaking. A 60 mL portion of the culture was then evenly distributed among four 6 L Erlenmeyer flasks to inoculate 16 L of LB media containing 50 μ g/mL kanamycin, 100 μ g/mL ampicillin, and 34 μ g/mL chloramphenicol, and was cultured further at 37 $^{\circ}$ C with shaking (180 rpm). At an optical density (600 nm; OD₆₀₀) of 0.3, solid arabinose was added to each flask at a final concentration of 0.2 % (w/v). At an OD₆₀₀ of 0.6 solid IPTG and ferric chloride were added to each flask at final concentrations of 400 and 50 μ M, respectively. The cultures

were then allowed to incubate further at 37 °C with shaking for 4 h. Cells were harvested at $10,000 \times g$ for 10 min at 4 °C with typical yields of 50-60 g frozen cell paste, which was frozen in liquid N₂ and stored at -80 °C until ready for use.

Purification of P. horikoshii NadA

Protein purification was carried out at room temperature by immobilized metal affinity chromatography using a nickel-nitrilotriacetic acid (Ni-NTA) matrix. In a typical purification, 25 g of frozen cells were resuspended in 80 mL of buffer A (50 mM HEPES, pH 7.5, 0.3 M KCl, 20 mM imidazole, and 10 mM 2-mercaptoethanol). Solid egg white lysozyme was added to a final concentration of 1 mg mL⁻¹ and the mixture was stirred at room temperature for 30 min. The suspended cells were heated at 37 °C for 15 min, then subjected to 4 cycles of a 1 min burst of sonic disruption (setting 7) followed by cooling to <8°C in an ice-water bath. Following sonication, 2M sodium sulfate solution was added to a concentration of 0.2 M, and the resulting solution was heated at 85 °C for 15 min. Cellular debris was removed by centrifugation at $50,000 \times g$ for 1 h, and the supernatant was loaded onto a Ni-NTA column (2.5 x 7 cm) equilibrated in buffer A. The column was washed with an additional 100 mL of buffer A before eluting with buffer A containing 250 mM imidazole. Fractions that were brown in color were pooled and concentrated in an Amicon stirred cell (Millipore, Billerica, MA) fitted with a YM-10 membrane (10,000 Da MW cutoff). The protein was exchanged into buffer B (50 mM HEPES, pH 7.5, 0.1 M KCl, 10 mM DTT, and 20% glycerol) by anaerobic gel filtration (Sephadex G-25), concentrated, and stored in aliquots in a liquid N₂ dewar until ready for use, or immediately reconstituted (see below) with iron and sodium sulfide.

Expression of Pyrococcus horikoshii Apo-NadA

Pyrococcus horikoshii NadA lacking an [4Fe-4S] cluster was produced by addition of *o*-phenanthroline to the growth media [14]. Cultures were initially grown as described above; however induction of the genes on plasmid pDB1282 was omitted. At an OD₆₀₀ of 0.6, 100 mM *o*-phenanthroline in 100 mM HCl was added to a final concentration of 100 μM. The cultures were then incubated for 15 min before induction with IPTG to a final concentration of 400 μM. Following induction, the cultures were incubated further for 4 h at 37 °C with shaking. Cells were harvested at 10,000 × *g* for 10 min at 4 °C, and the cell paste was frozen in liquid N₂ and stored at -80 °C until ready for use.

Purification of Pyrococcus horikoshii Apo-NadA

Apo-NadA was purified using the method described for holoprotein. Eluted protein was detected by reaction with Coomassie blue dye-binding reagent.

Reconstitution of NadA

Reconstitution of NadA with iron and sulfide was carried out at ambient temperature in a Coy anaerobic chamber using anaerobic buffers and solutions. A typical reconstitution contained, in a final volume of 20 mL, 100 μM NadA that was initially treated with 5 mM DTT for 2 hours. Then an 8-fold molar excess of FeCl₃ was added and the solution was allowed to sit on ice for 20 min. Finally, an 8-fold molar excess of Na₂S was added over the period of 3 to 4 h, which was followed by incubation for 13 h. The solution was then concentrated in an Amicon stirred cell, placed in airtight centrifuge tubes, removed from the anaerobic chamber, and centrifuged at 14,000 × *g* for 2 min to remove precipitate. The RCN samples were brought back into the anaerobic chamber,

and the supernatants were removed and exchanged into buffer C by gel filtration (Sephadex G-25 or Amersham PD-10), reconcentrated, and stored in aliquots in a liquid N₂ dewar.

Determination of Protein Concentration

Protein concentrations were determined by the Bradford dye staining procedure with BSA as the standard [15]. *Pyrococcus horikoshii* NadA was subjected to quantitative amino acid analysis at the University of California Davis Molecular Structure Facility to determine that the Bradford method overestimates the true *P. horikoshii* NadA concentration by a factor of 1.54.

Assay for Quinolinic Acid

The activity of NadA was determined by monitoring the formation of QA over a 20 min time period under anaerobic conditions. The isolated enzyme was found to exhibit optimal activity at a temperature of 50 °C, and pH of 7.0. The substrate IA was generated chemically by reacting OAA with ammonium chloride [1]. The assay contained, in a final volume of 1700 µL, 200 mM HEPES, pH 7.0, 1 mM DHAP, 0.3 mM L-tryptophan (internal standard), 10 mM OAA, 100 mM ammonium chloride, and 10 µM NadA. The reactions were initiated by addition of OAA after incubation of the other components in the assay mixture at 50 °C for 5 min. At designated times, 200 µL aliquots of the assay mixture were removed and added to 40 µL of 2 M trichloroacetic acid to quench the reaction. The precipitated protein was pelleted by centrifugation and the supernatant was analyzed by HPLC with UV detection (268 nm) using a Zorbax SB-C18 column (4.6 x 250 mm), which was obtained from Agilent. The column was equilibrated in 100% Solvent A (1% TFA) at a flow rate of 1 mL min⁻¹. These initial

conditions were maintained for 10 min after injection, after which a gradient of 0-45% Solvent B (acetonitrile) was applied over 10 min. At 20 min, a gradient of 45-90% Solvent B was applied over 3 min. Finally, at 25 min, a gradient of 90-0% Solvent B was applied over 3 min to re-establish the initial conditions until the end of the run at 32 min. Using this method, QA acid eluted at 8.3 min and the tryptophan internal standard eluted at 20.3 min. The concentration of QA was determined from a calibration curve of known concentrations of QA, using the internal standard to correct for volume changes between sample injections.

Preparation of Mössbauer and EPR Samples

In order to analyze samples by Mössbauer spectroscopy, pET28a containing *P. horikoshii nadA* and pDB1282 were transformed into *E. coli* BL21(DE3) cells, which were cultured in M9 minimal media without chloramphenicol. In addition, $^{57}\text{FeSO}_4$ was substituted for FeCl_3 . All other growth and purification procedures were as described above. Mössbauer samples (400 μL total volume) were prepared in small plastic cups before freezing in liquid N_2 . EPR samples (250 μL total volume) of reduced *P. horikoshii* NadA were treated with 2 mM sodium dithionite at room temperature for approximately 5 min prior to loading them in EPR tubes (2 mm i.d.) and freezing in liquid N_2 . Samples analyzed contained 425-950 μM NadA and were all prepared inside of the anaerobic chamber.

Crystallization

Crystallization of *P. horikoshii* NadA was performed at the X-ray Crystallography Facility at The Pennsylvania State University, University Park. Conditions were optimized using Hampton Pre-Crystallization Test (PCT) and screening kits used in

conjunction with the Artrobbins Instruments Phoenix protein crystallization robot. Using the sitting drop vapor diffusion method, a brown, rod-shaped crystal was obtained after 14 days at 10 °C using a 1:1 ratio of 10 mg/mL protein solution containing the substrate mimic malate, and a buffer of 0.1 M sodium acetate, pH 5.5, with 2.7 M ammonium sulfate. Dynamic light scattering was performed using a Viscotek 802 Dynamic Light Scattering Instrument with the associated Omnisize software program.

4.3 Results

Expression of P. horikoshii NadA

The *P. horikoshii* NadA gene was cloned into an IPTG-inducible pET28a vector such that the resulting protein would contain an N-terminal hexahistidine tag, and cotransformed into *E. coli* BL21 (DE3) Rosetta2 cells along with the arabinose-inducible plasmid pDB1282 containing the *A. vinelandii* *isc* operon. Although induction of the *isc* proteins is not seen by SDS-PAGE, NadA is clearly produced during a 4 h induction at 37 °C, as shown by the band of molecular mass ~35 kDa (Figure 4-2, Lane 4). The resulting cell paste was brown in color, and obtained in a yield of ~1.5 g per liter of media.

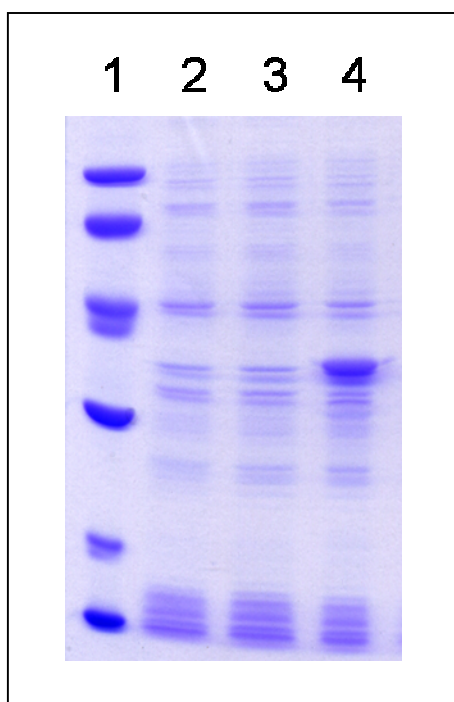


Figure 4-2: SDS-PAGE of *P. horikoshii* NadA expression
 Lane 1: molecular weight standards (from top); 97.0, 66.0, 45.0, 30.0, 20.1, 14.4 kDa;
 Lane 2: at OD₆₀₀ 0.3; Lane 3: at OD₆₀₀ 0.6; Lane 4: after 4 hour induction

Purification and Characterization of P. horikoshii NadA

P. horikoshii NadA was successfully isolated under anaerobic conditions as described in Materials and Methods. The protein was highly soluble, with very little apparent in the pellet after centrifugation (Figure 4-3, lane 3). The final protein, which was obtained in a yield of ~10 mg per gram of cell paste, was dark brown in color and essentially homogeneous as determined by SDS-PAGE (Figure 4-3, lane 6). The UV-visible spectral envelope was consistent with the presence of a [4Fe-4S] cluster (Figure 4-4, solid line); the spectrum contained a shoulder at ~320 nm, a peak at ~400 nm, and broad tailing that extended beyond 700 nm. Iron and sulfide quantification of this protein indicated the presence of 2.3 ± 0.4 equivalents of the former, and 2.6 ± 1.0 of the latter per polypeptide, similar to those found for the AI *E. coli* enzyme [3]. Chemical reconstitution of the AI protein resulted in an increase in the UV-visible absorbance at

400 nm (Figure 4-4, dashed line) as well as iron and sulfide content, which was present at 5.8 ± 0.1 equiv and 4.4 ± 0.1 equiv per polypeptide, respectively. These numbers are consistent with the presence of one [4Fe-4S] cluster per polypeptide, as previously found for the *E. coli* [3] and *M. tuberculosis* proteins (unpublished results).

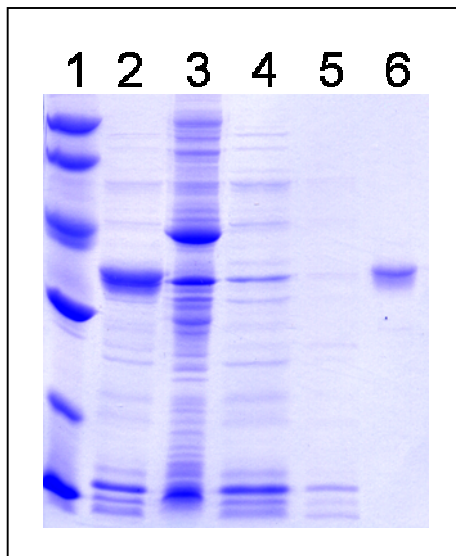


Figure 4-3: SDS-PAGE of *P. horikoshii* NadA purification

Lane 1: molecular weight standards (from top); 97.0, 66.0, 45.0, 30.0, 20.1, 14.4 kDa;
Lane 2: lysate supernatant; Lane 3: lysate pellet; Lane 4: Ni-NTA load eluate; Lane 5:
Ni-NTA wash eluate; Lane 6: purified protein

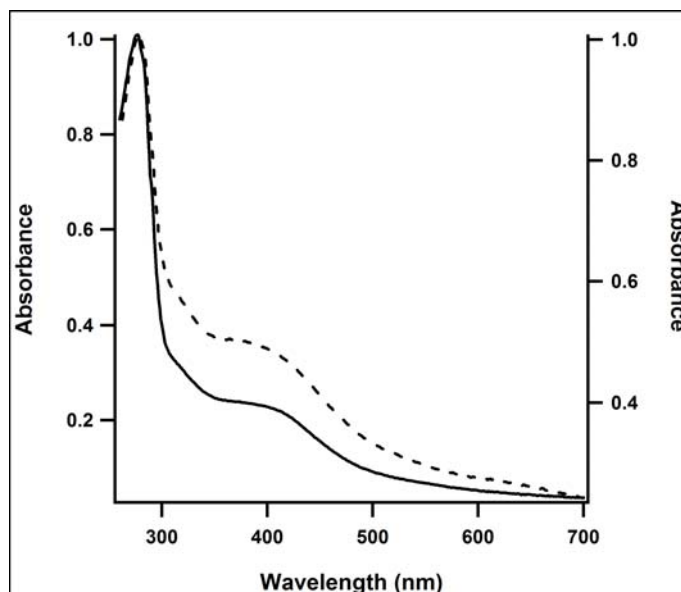


Figure 4-4: UV-visible spectra of WT *Pyrococcus horikoshii* NadA, AI (solid line, left axis), and RCN (dashed line, right axis).

The optimum activity of NadA was seen at a pH of 7.0 and temperature of 50 °C, which was used for all subsequent assays. As-isolated protein catalyzed the formation of QA at 50 °C with a $V_{\max}/[E_T]$ of 1.89 min^{-1} , while RCN enzyme displayed a $V_{\max}/[E_T]$ of 3.18 min^{-1} . This specific activity, $\sim 0.1 \text{ } \mu\text{mol min}^{-1} \text{ mg}^{-1}$, is significantly less than that previously reported by Sakuraba [6]. However, when it was purified under aerobic conditions, as described by Sakuraba et. al., it was completely inactive.

To ensure that the heat treatment used in the procedure did not affect formation of the cluster, NadA was also purified with elimination of the heat treatment steps from the purification scheme above. The heat treatment did not have a negative effect, as the activity, iron and sulfide stoichiometry, EPR, Mössbauer and UV-visible spectra were all similar to that of the heat-treated protein.

Mössbauer and EPR Spectroscopy of P. horikoshii NadA

P. horikoshii NadA was also produced in the presence of the isotope ^{57}Fe , allowing for further study by Mössbauer spectroscopy. The 4.2 K Mössbauer spectrum recorded in a parallel magnetic field of 40 mT showed the expected quadrupole doublet for a $[\text{4Fe-4S}]^{2+}$ cluster, with a quadrupole splitting parameter (ΔE_Q) of 1.19 mm/s and isomer shift (δ) of 0.43 mm/s, accounting for approximately ~87% of the signal (Figure 4-5, data indicated by black hashes, fit indicated by solid line). Unexpectedly, there is a second quadrupole doublet accounting for approximately 13% of the spectrum, which could be simulated with a ΔE_Q of 1.53 mm/s and isomer shift of 0.82 mm/s (Figure 4-5, dashed line). The source of the minor quadrupole doublet is unknown, but the large isomer shift suggests that it may be the result of multidentate binding of an organic molecule with hard N/O donor atoms at the unique Fe_a site of the Fe/S cluster, as previously observed for aconitase [15] and pyruvate formate-lyase activase, [16] two other $[\text{4Fe-4S}]$ cluster proteins. and is currently under further investigation. The signal was not increased by EPR spectroscopy of the protein reduced with 2 mM dithionite and recorded at 5 mW power and 13 K exhibited a weak rhombic spectrum, but was similar to that seen for reduced AI wild-type *M. tuberculosis* NadA, with g values of 1.94, and 2.10 (Figure 4-6).

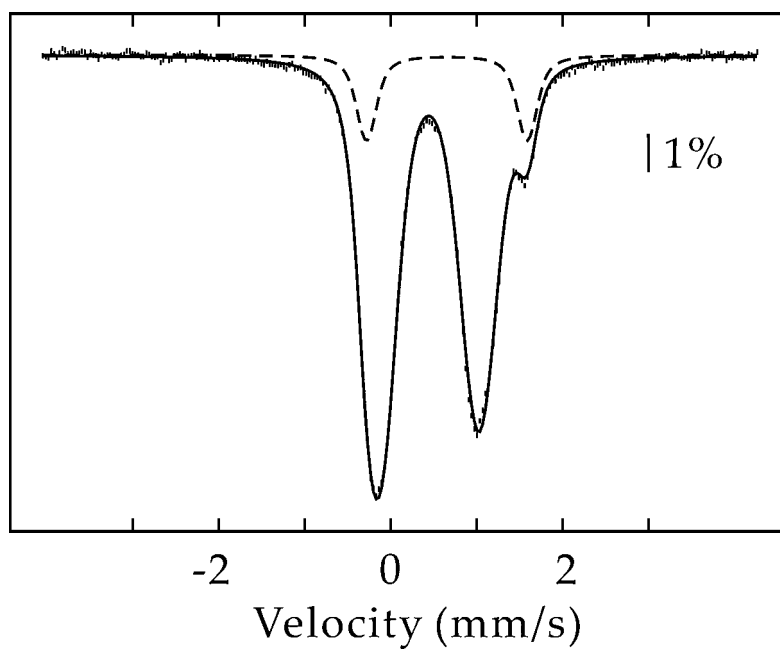


Figure 4-5: Mössbauer spectrum of as-isolated ^{57}Fe *P. horikoshii* NadA

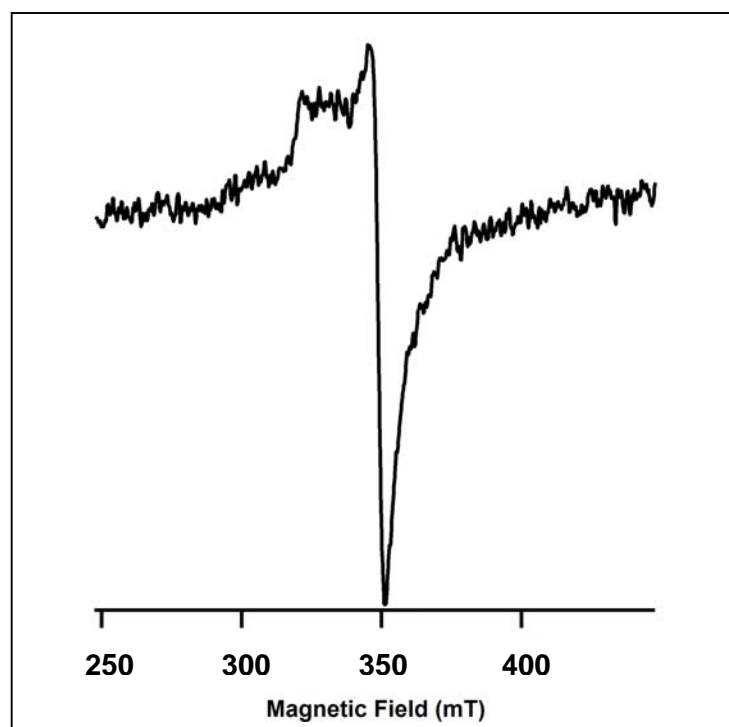


Figure 4-6: EPR spectrum of reduced as-isolated ^{57}Fe *P. horikoshii* NadA

Expression, Purification and Characterization of P. horikoshii NadA Apoprotein

To demonstrate the necessity of the cluster for catalysis, cluster-less apoprotein was produced by adding the iron-chelator, *o*-phenanthroline, to the growth media prior to induction. This method had been successful at producing the apo- form of the dinuclear iron protein ribonucleotide reductase [13], and the *E. coli* NadA protein. Expression and purification of the apoprotein appeared similar to that of the holoprotein when viewed by SDS-PAGE. However, the cell pellet obtained after harvesting was light tan in color, and the isolated protein was colorless. As expected, the UV-visible spectrum of the apoprotein contained no features other than the typical protein absorption at 280 nm (Figure 4-7, solid line). After chemical reconstitution and gel filtration, the typical brown color of the protein was restored, as well as the broad absorbance at 400 nm (Figure 4-7, dashed line). Most importantly, while the apoprotein had no observable quinolinate synthase activity (Figure 4-8, black circles), the reconstituted form had a $V_{\max}/[E_T]$ of 3.31 min^{-1} , similar to that of the reconstituted holoprotein (Figure 4-8, red squares). In addition, it was found that the inactive, aerobically isolated holoprotein could also be chemically reconstituted anaerobically in the same manner, and form fully active protein (results not shown).

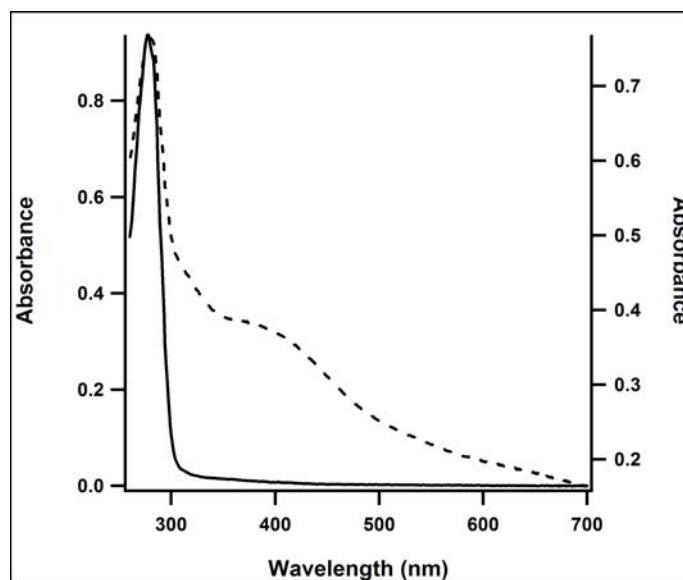


Figure 4-7: UV-visible spectra of AI (solid line, left axis) and RCN (dashed line, right axis) Apo-NadA from *Pyrococcus horikoshii*.

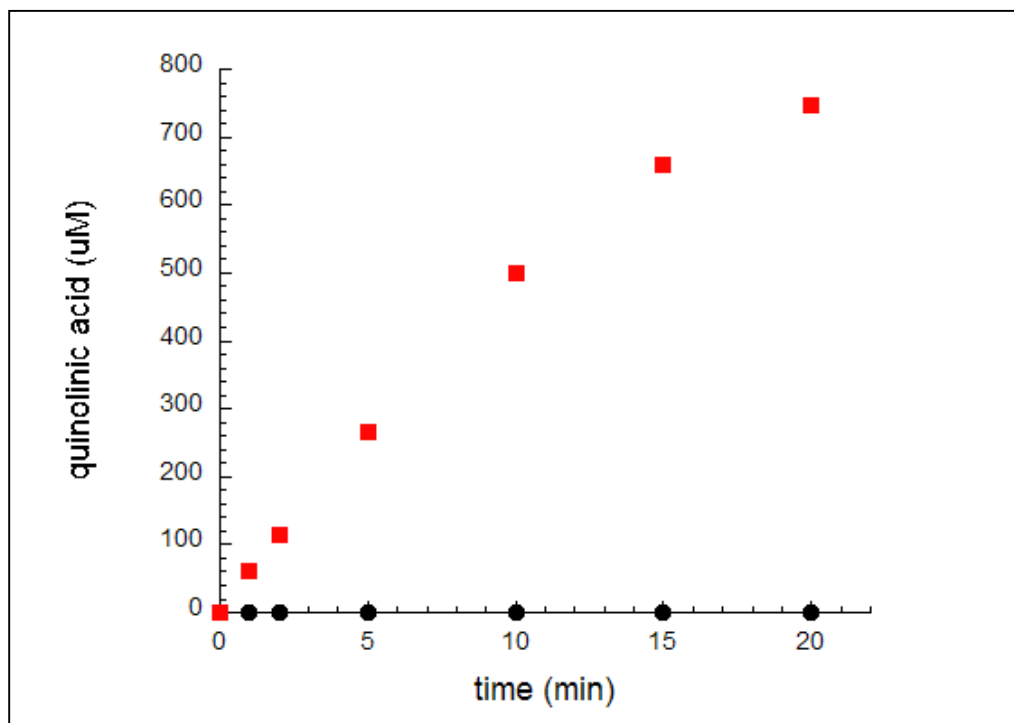


Figure 4-8: Quinolinic acid formed by apo-NadA as-isolated (black circles), and after chemical reconstitution (red squares).

Dynamic Light Scattering of P. horikoshii NadA

Prior to crystallization attempts, the purity of the protein was assessed by SDS-PAGE and dynamic light scattering (DLS). Using the latter technique, a protein solution is submitted to a beam of monochromatic light, which undergoes a doppler shift relative to the size of the protein in solution. Using a 2 mg/mL sample of *P. horikoshii* in the absence of substrate indicated that the sample for crystallization contained only one species with an average diameter of 2.7 nm. Assuming a spherical distribution, this predicts a molecular mass of 35.1 kDa for the protein, in agreement with the previously published molecular mass.

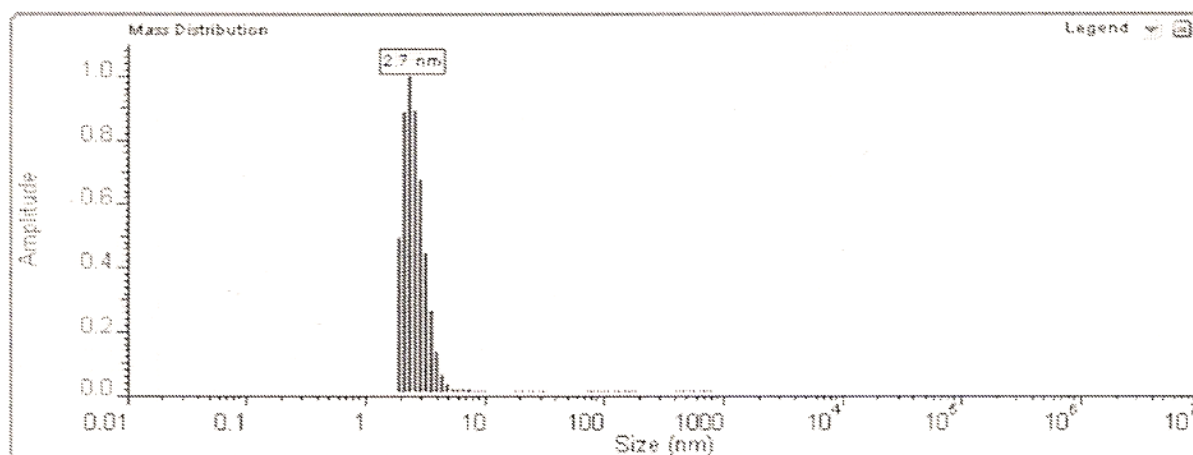


Figure 4-9: Average diameter plot obtained from DLS of *P. horikoshii* NadA

Crystallization of P. horikoshii NadA

Prior to crystallization screenings, *P. horikoshii* NadA was incubated at various temperatures in the presence of various combinations of substrates and substrate mimics, and monitored spectroscopically for 10 days. Based on the UV-visible absorbance of the protein at 400 nm, it appeared that the presence of the substrate aspartate was effective in preventing oxidative degradation of the cluster. Use of the Hampton PCT kit determined a protein concentration of 10 mg/mL and temperature of 10 °C to be optimal for

crystallization. Therefore, wide-scale screening was performed aerobically at 10 °C using Hampton kits and 10 mg/mL protein. In addition, screening was performed with NadA incubated with a 100-fold excess of the substrate aspartate, or the substrate mimic malate, which was found to be necessary for crystallization in the previously solved structure [6]. Crystallization was performed using the sitting drop vapor diffusion method, and plates were examined every few days. A brown rod-shaped crystal was obtained after 14 days at 10 °C using a 1:1 ratio of 10 mg/mL protein solution containing the substrate mimic malate, and a buffer of 0.1 M sodium acetate, pH 5.5, with 2.7 M ammonium sulfate.

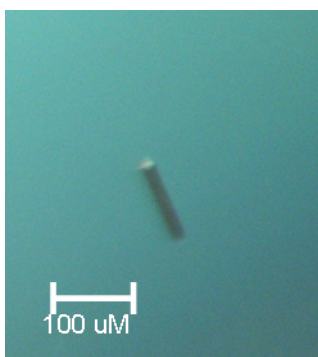


Figure 4-10: Crystal of *P. horikoshii* NadA

4.4 Discussion

The gene for *P. horikoshii* NadA was successfully cloned into a pET28 vector such that the protein would contain an N-terminal hexahistidine tag, allowing for a simple large-scale purification scheme. Minimal production of the protein was observed in the BL21 (DE3) cell line; therefore, the *nadA* gene was subsequently transformed into the Rosetta2 cell line, which encodes seven rare tRNAs. Expression in the Rosetta2 cell line

allowed suitable protein production, as shown in lane 4 of Figure 4-2. Coexpression of genes encoding Fe/S proteins with those on plasmid pDB1282, which encodes Fe/S cluster assembly proteins, has been used successfully by the Booker lab to isolate proteins with intact clusters [17]. In this case, induction of the genes on pDB1282 did not result in a visible change in production of the Isc proteins (Figure 4-2, lane 3). However, this has also been observed with NadA proteins from other organisms studied in the Booker lab.

The anaerobically isolated NadA protein was dark brown in color. Iron and sulfide quantification, in addition to UV-visible, EPR, and Mössbauer spectroscopies, established that the *P. horikoshii* NadA protein contained one $[4\text{Fe-4S}]^{2+}$ cluster per polypeptide. In addition, the *P. horikoshii* NadA protein behaved nearly identically to those from *E. coli* [3] and *M. tuberculosis* (unpublished data). Although there was no cluster found in the solved crystal structure, nor mention of an Fe/S cluster as a possible cofactor in the paper by Sakuraba *et.al*, the work described herein clearly demonstrates that it is a required cofactor. The lack of cluster in the crystallized protein is most likely the result of oxidative degradation caused by purification of the protein under aerobic conditions. Observations made in the Booker lab indicate that the cluster is very sensitive to oxygen, and much more so than the *E. coli* or *M. tuberculosis* NadA proteins.

Isolation of the cluster-less apoprotein by addition of *o*-phenanthroline to the growth media confirmed that the cluster is in fact necessary for catalysis. While the catalytically competent protein forms QA with a $V_{\text{max}}/[E_T]$ of 1.89 min^{-1} , the apoprotein did not generate any observable QA after 20 mins, with $5 \mu\text{M}$ being the limit of detection in the HPLC assay used. The same protein was chemically reconstituted, and found to

have iron and sulfide content as well activity that is nearly identical to that of reconstituted holoprotein. Therefore, activity of the protein is entirely dependent on the presence of the [4Fe-4S] cluster.

These results from the Booker lab call into question the reported specific activity of *P. horikoshii* NadA of $2.2 \mu\text{mol min}^{-1} \text{mg}^{-1}$ by Sakuraba et al., which is over 20-fold higher than the values reported herein. Comparison of the assay techniques between the two groups reveals several differences. In the report by Sakuraba et al, the substrate IA is generated by NadB. The Booker lab routinely uses IA generated artificially from Schiff base formation between OAA and an ammonia source as described by the work of Gholson [1]. However, this difference does not account for the disparity in activity numbers. In the HPLC assay used by the Booker lab to monitor QA formation, detection is made at 268 nm, the λ_{max} of QA. However, Sakuraba et al. monitor product formation at 254 nm, the λ_{max} at which OAA absorbs light. Moreover, a peak that displays a maximum absorbance at 254 nm is routinely observed by the Booker lab to increase as a function of time in assays containing NadB, and is found at the same retention time in assays containing OAA and an ammonia source. Therefore, it appears that the numbers reported by Sakuraba et al. are for OAA or IA rather than QA. Iminoaspartate is unstable, with a half-life of 2.5 mins at 37 °C. Therefore over the course of an assay, increasing amounts of IA will be hydrolyzed to OAA and ammonia, resulting in an observed increase in the amount of OAA, the side-product probably detected by Sakuraba et al [1].

The final goal of this work is to obtain the first complete structure of a quinolinate synthase in order to gain insight into the mechanism of catalysis and the manner in which

active site amino acids are used in the reaction. As an initial step in this work, several substrates or substrate mimics were found to have a protective role in preventing oxidative degradation of the cluster, allowing wide-scale crystallization screenings to be set up aerobically. Although a crystal was formed, its brown color suggesting the presence of an Fe/S cluster, this small crystal was not of diffraction quality, and crystallization of the protein has not been reproduced. The crystals obtained by Sakuraba et al were produced after several rounds of crystal seeding, and only in the presence of the substrate mimic malate. The presence of an intact cluster should facilitate crystallization by anchoring the cysteine-containing loop regions and thereby providing a more static structure, allowing a complete structure with cluster to be resolved.

An image of the active site of the protein will provide a structural foundation for future biochemical studies providing information on the catalytic mechanism of quinolinate synthase and the class of cluster-containing hydro-lyases as a whole. Our hypothesis is that the cluster will serve as a Lewis acid, coordinating the QA precursor through its hydroxyl group prior to elimination. To date, this role has only been extensively studied in aconitase, which binds substrate in a different manner, and catalyzes a more complex set of reactions. Therefore, the NadA crystal structure will provide information about not only quinolinate synthases, but also the hydro-lyases, as a prime example of Fe/S clusters serving essential catalytic roles.

4.5 References

1. Nasu, S., and Gholson, R. K. (1981) Replacement of the B protein requirement of the *E. coli* quinolinate synthetase system by chemically-generated iminoaspartate. *Biochem. Biophys. Res. Commun.* 10, 533-539.
2. Flint, D. H., Allen, R. M. (1996) Iron-sulfur proteins with nonredox functions. *Chem Rev* 96, 2315-2234.
3. Cicchillo, R. M., Tu, L., Stromberg, J. A., Hoffart, L. M., Krebs, C., and Booker, S. J. (2005) *Escherichia coli* quinolinate synthetase does indeed harbor a [4Fe-4S] cluster. *J. Am. Chem. Soc.* 127, 7310-7311.
4. Ollagnier-de Choudens, S., Loiseau, L., Sanakis, Y., Barras, F., and Fontecave, M. (2005) Quinolinate synthetase, an iron-sulfur enzyme in NAD biosynthesis. *FEBS Lett.* 579, 3737-3743.
5. Ceciliani, F., Caramori, T., Ronchi, S., Tedeschi, G., Mortarino, M., and Galizzi, A. (2000) Cloning, overexpression, and purification of *Escherichia coli* quinolinate synthetase. *Prot. Express. Purif.* 18, 64-70.
6. Sakuraba, H., Tsuge, H., Yoneda, K., Katunuma, N., and Ohshima, T. (2005) Crystal structure of the NAD biosynthetic enzyme quinolinate synthase. *J. Biol. Chem.* 280, 26645-26648.
7. Beinert, H. (1978) Micro methods for the quantitative determination of iron and copper in biological material. *Methods Enzymol.* 54, 435-445.
8. Beinert, H. (1983) Semi-micro methods for analysis of labile sulfide and of labile sulfide plus sulfane sulfur in unusually stable iron-sulfur proteins. *Anal. Biochem.* 131, 373-378.

9. Kennedy, M.C., Kent, T. A., Emptage, M., Merkle, H., Beinert, H., and Münck, E. (1984) Evidence for the formation of a linear [3Fe-4S] cluster in partially unfolded aconitase. *J. Biol. Chem.* 259, 14463-14471.
10. Kriek, M. M., Peters, L. L., Takahashi, Y. Y., and Roach, P. L. (2003) Effect of iron-sulfur cluster assembly proteins on the expression of *Escherichia coli* lipoic acid synthase, *Prot. Express. Purif.* 28, 241-245.
11. Frazzon, J., Fick, J. R., and Dean, D. R. (2002) Biosynthesis of iron-sulphur clusters is a complex and highly conserved process. *Biochem. Soc. Trans.* 30, 680-685.
12. Frazzon, J., and Dean, D. R. (2003) Formation of iron-sulfur clusters in bacteria: an emerging field in bioinorganic chemistry. *Curr. Opin. Chem. Biol.* 7, 166-173.
13. Parkin, S. E., Chen, S., Ley, B. A., Mangravite, L., Edmondson, D. E., Huynh, B. H., and Bollinger, J. M., Jr. (1998) Electron injection through a specific pathway determines the outcome of oxygen activation at the diiron cluster in the F208Y mutant of *Escherichia coli* ribonucleotide reductase. *Biochemistry* 37, 1124-1130.
14. Bradford, M. M. (1976) A rapid and sensitive method for the quantitation of microgram quantities of protein utilizing the principle of protein-dye binding. *Anal. Biochem.* 72, 248-254.
15. Kent, T. A., Emptage, M. H., Merkle, H., Kennedy, M. C., Beinert, H., and Münck, E. (1983) Mössbauer and EPR studies of activated aconitase: Development of a localized valence state at a subsite of the [4Fe-4S] cluster on binding of citrate. *Proc. Natl. Acad. Sci. USA* 80, 4674-4678.

16. Krebs, C., Broderick, W. E., Henshaw, T. F., Broderick, J. B., and Huynh, B. H. (2002) Coordination of adenosylmethionine to a unique iron site of the [4Fe-4S] of pyruvate formate-lyase activating enzyme: a Mössbauer spectroscopic study. *J. Am. Chem. Soc.* *124*, 912-913.
17. Cicchillo, R. M., Lee, K., Baleanu-Gogonea, C., Nesbitt, N. M., Krebs, C., and Booker, S. J.. (2004) *Escherichia coli* lipoyl synthase binds two distinct [4Fe-4S] clusters per polypeptide. *Biochemistry* *43*, 11770-11781.